**EOARD Project SPC 01-4082:**
**Contract order number: F61775-01-C0011**

# Helical Large-Core Fiber Lasers

# Final Report

W. A. Clarkson, P. Wang, L. J. Cooper, J. K. Sahu
Optoelectronics Research Centre
University of Southampton
Southampton, SO17 1BJ
United Kingdom

# REPORT DOCUMENTATION PAGE

Form Approved OMB No. 0704-0188



| 1. REPORT DATE *(DD-MM-YYYY)* | 2. REPORT TYPE | 3. DATES COVERED *(From – To)* |
|---|---|---|
| 27-06-2005 | Final Report | 28 September 2001 - 28-Sep-03 |

**4. TITLE AND SUBTITLE**

Helical Large-Core Fiber Lasers

**5a. CONTRACT NUMBER**
F61775-01-C0011

**5b. GRANT NUMBER**

**5c. PROGRAM ELEMENT NUMBER**

**6. AUTHOR(S)**

Dr. William A Clarkson

**5d. PROJECT NUMBER**

**5d. TASK NUMBER**

**5e. WORK UNIT NUMBER**

**7. PERFORMING ORGANIZATION NAME(S) AND ADDRESS(ES)**
University of Southampton
Southampton SO17 1BJ
United Kingdom

**8. PERFORMING ORGANIZATION REPORT NUMBER**

N/A

**9. SPONSORING/MONITORING AGENCY NAME(S) AND ADDRESS(ES)**

EOARD
PSC 802 BOX 14
FPO 09499-0014

**10. SPONSOR/MONITOR'S ACRONYM(S)**

**11. SPONSOR/MONITOR'S REPORT NUMBER(S)**
SPC 01-4082

**12. DISTRIBUTION/AVAILABILITY STATEMENT**

Approved for public release; distribution is unlimited.

**13. SUPPLEMENTARY NOTES**

**14. ABSTRACT**

This report results from a contract tasking University of Southampton as follows: The contractor will investigate a simple alternative approach for selecting the polarization of light transmitted through an optical fiber, based on the use of a fiber with a core (transmitting region) that has a helical (corkscrew) trajectory along the fiber. This should allow the use of fibers with a larger core area, capable of transmitting more power, while maintaining good control of the light distribution in the fiber. The project will examine ways to produce helical-core fibers, will test their properties for light propagation, will develop and test alternative designs and will deliver samples of helical-core optical fiber lasers.

**15. SUBJECT TERMS**
EOARD, Fibre Optics, Lasers, Fibre Lasers

| 16. SECURITY CLASSIFICATION OF: | | | 17. LIMITATION OF ABSTRACT | 18, NUMBER OF PAGES | 19a. NAME OF RESPONSIBLE PERSON |
|---|---|---|---|---|---|
| a. REPORT | b. ABSTRACT | c. THIS PAGE | | | DONALD J SMITH |
| UNCLAS | UNCLAS | UNCLAS | UL | 41 | 19b. TELEPHONE NUMBER *(Include area code)* +44 (0)20 7514 4953 |

# Contents:

## 1.0 Introduction

Over the last decade there has been growing interest in cladding-pumped fiber lasers and amplifiers as a means for generating high output powers. The main attractions of fiber lasers are derived directly from their geometry, which allows relatively simple thermal management with waste heat distributed over a long length of fiber reducing the likelihood of damage. Moreover, the output beam quality is determined by the waveguiding properties of the active-ion-doped core, which can be tailored to produce a single-mode output beam. However, scaling to very high power levels requires double-clad fibers with a much larger core area than standard single-mode cores in order to avoid the need for excessively long fibers for efficient pump absorption, and to raise the threshold for unwanted nonlinear processes and optical damage. This is generally achieved by employing a multimode large-mode-area core design with a low numerical aperture in combination with bend loss suppression of higher-order modes [1] to promote single-mode operation. Using this approach, single-mode powers >500W in the ~1μm regime have recently been demonstrated from a cladding-pumped Yb-doped fiber laser with a core diameter of 24.5μm (NA = 0.086) and an inner-cladding size of ~400μm [2], and single-mode powers >1kW from a cladding-pumped Yb-doped fiber laser with a core diameter of 40μm (NA <0.05) and an inner-cladding size of ~650μm [3]. These results serve as an impressive demonstration of the power-scaling potential of fiber lasers. However, scaling single-mode operation to even higher power levels will require an even larger core diameter and a larger inner-cladding diameter to facilitate in-coupling more pump power, making it increasingly difficult to use bend loss filtering as an effective means for suppressing higher-order modes.

The main aim of this research program was to investigate an alternative approach for achieving robust single-mode operation in a large-core fiber laser or amplifier based on the use of a fiber with a helical core trajectory within the inner-cladding.

## 2.0 Objectives

Helical-core fibers have a number of attractive features for power-scaling of fiber lasers (see figure 1): The offset-core helps to promote efficient pump absorption in a cladding-pumped fiber configuration. The ‘helical’ loss due to the core trajectory is greater for higher-order modes, and hence can be used as a very effective means for suppressing high order modes in a in a large-core fiber device without resort to bending. Moreover, helical-core fibers, due to their geometry, exhibit circular birefringence which, with appropriate design, can be made large enough for maintaining linearly-polarized or circularly-polarized propagation of laser radiation in a fiber laser or amplifier. The above features suggest that helical-core fibers have a great deal of promise as a ‘power scalable’ fiber architecture. The overall objective of this program of work was to explore the parameter space to see if these advantages could be realised in practical helical-core fiber device.

The specific objectives of the research program were as follows:

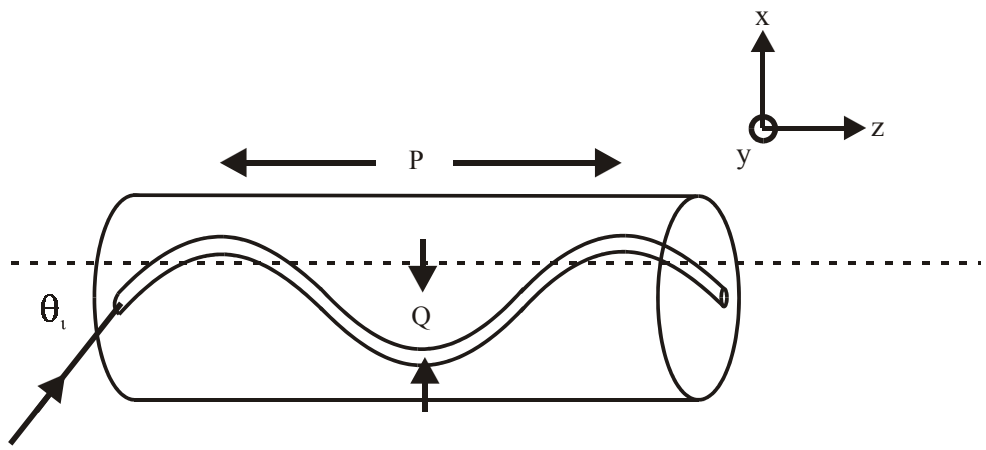


Figure 1: Helical-core fiber with core offset, Q, pitch, P, and pitch angle, $\theta_i$ .

(a) Establish a method for fabrication capability for helical core fibers and fabricate helical-core fibers with a range of pitches, core-offsets and core sizes. and to investigate the "distributed mode filter" function of the yb-doped helical core fiber.

(b) Investigate the properties (i.e. propagation loss, circular birefringence) of undoped helical core fibers with the aim of developing a strategy for the design of rare-earth-ion doped helical-core fibers for use in laser/amplifier configurations.

(c) Develop a high-power diode-stack pump module and coupling scheme for pumping helical-core fiber lasers and amplifiers, and evaluate its performance by cladding pumping a simple straight (offset-core) Yb-doped fiber laser.

(d) Demonstrate a core-pumped Yb-doped helical-core fiber laser

(e) Develop a quantitative model for estimating the propagation losses in helical-core fibers as a design aid for high-power laser/amplifier devices.

(f) Demonstrate high-power cladding-pumped Yb-doped helical-core fiber lasers and amplifiers.

(g) Consider the prospects for further power scaling and the future potential for helical-core fiber devices.

## 3.0 Fabrication of helical-core fibers

Helical-core fibers were investigated in the late 1980's with intended applications in sensors, but to the best of our knowledge the use of an active-ion-doped helical-core fiber in a laser configuration had not been demonstrated. In the early stages of this project our efforts were directed towards establishing a fabrication capability for helical-core fibers.

Helical-core fibers can be made by spinning a preform with an offset core during the fiber drawing process. To fabricate helical-core fibers we therefore constructed a preform spinning system and installed it on the fiber pulling tower. The spinning system could be operated at a maximum rotational speed of up to 2000 rpm. In early trial fabrication runs it was evident that careful alignment of the preform axis to the rotation axis was necessary to avoid any distortion in the preform during spinning and to minimise the chance of the fiber breaking.

We have investigated two different approaches for fabricating the offset-core preform (as shown in figure 2). The first of these (illustrated in figure 2(a)) is the well-known 'rod-in-tube' method. In this approach the offset core obtained by drilling a hole in a solid glass cylinder (offset from the axis), and inserting a rod with the appropriate core design. This approach has the attraction that core-offset can be accurately specified, but the approach has the drawback that due to the limited drill length, the preform length is limited (in our case) to ~30cm. This obviously limits the length of fiber that can be drawn from the preform, and hence the approach is not well-suited to the production of fibers with large inner-cladding sizes. The alternative approach for producing an offset-core preform (illustrated in figure 2(b)) is the 'stacking' method. The procedure involves etching a standard preform to remove most of the cladding material, leaving the core plus a thin cladding region, and then carefully stacking the resulting rod inside a high

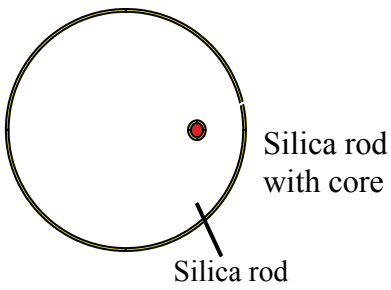


Figure 2(a): Rod-in-tube method

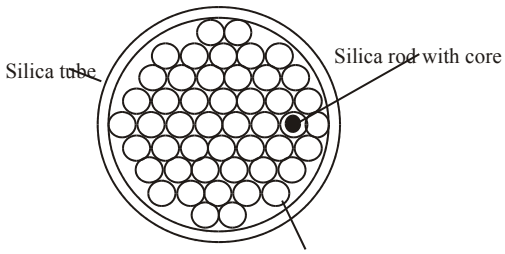


Figure 2(b): Stacking method

quality silica tube with a number of high quality silica rods. The rod containing the core is positioned so that it is offset from the axis. This approach has the advantage over rod-in-tube method, that much longer preforms are can be fabricated in a relatively simple manner. However, it has the disadvantage that it is difficult to precisely specify the offset distance, since, when the preform is heated up and collapsed to remove the air between the rods, there is usually

some movement of the core relative to the preform axis. This is not a serious problem since the position of the core relative to the preform axis can be measured and the pitch chosen so that the desired radius of curvature ($R=Q/\sin^2\theta_p$) of the core trajectory (and hence the required degree of mode filtering) can be obtained. However, it does mean that it is difficult to fabricate preforms (and hence fibers) with identical designs.

A number of trial fabrication runs were performed to identify the best method for drawing a fiber from the 'stacked' preform, so that all the air holes were removed during the preform collapse stage. It was found that at high spinning speeds the standard technique of simply drawing the preform on the pulling tower was not effective in removing all the air holes, so it was necessary to pre-collapse the preform using a fiber fabrication lathe, with careful optimization of the stacking pattern to minimize the air spaces between the stacked rods.

A number of further trial fabrication runs were performed with offset-core preforms fabricated in this manner, yielding helical-core fibers with a range of pitches and core offsets (with and without polymer outer-coatings) to test the limits of the system. Using this fabrication procedure we have successfully fabricated helical-core fibers with pitches as short as 1.8mm. A rough, but direct measurement of pitch can made by imaging the core of the fiber (over one section of its helical trajectory) on a CCD camera (as shown in Figure 3).

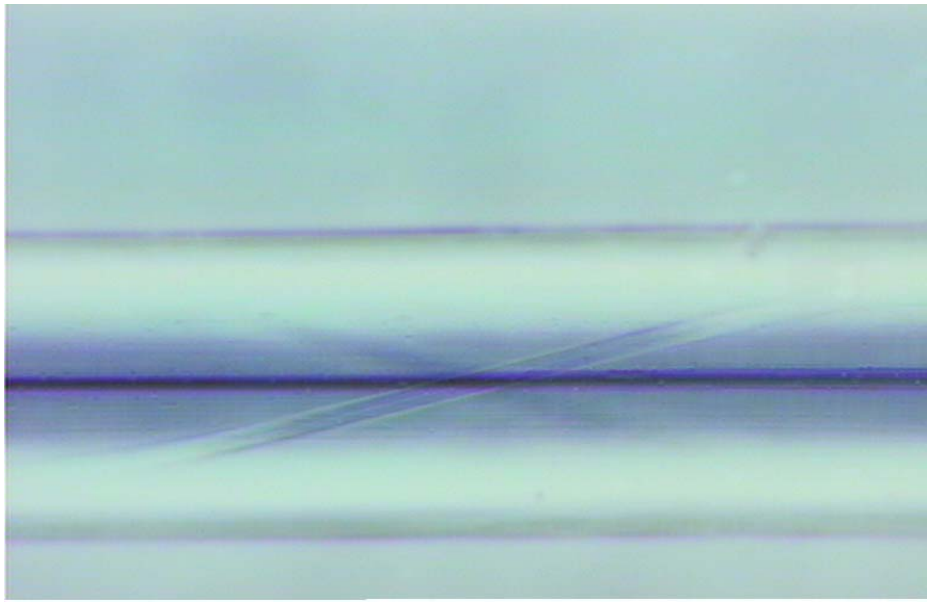

Figure 3. Photo of helical core fiber showing the core crossing the centre of the fiber.

The two main factors limiting the minimum pitch are the spinning speed and the drawing speed. Clearly, the slower the drawing speed the shorter the pitch. However, this makes it necessary to reduce the preform feed speed in order to maintain constant fiber diameter. The minimum preform feed speed is determined by the need for a smooth translation. At very low speeds it is difficult to maintain a smooth translation resulting in variations in the fiber diameter.

The pitch can also be decreased by increasing the preform spinning speed. The upper limit on spinning speed is determined by centripetal acceleration causing the hot glass in the drawing furnace to 'throw out' from the preform axis resulting damage to the fiber. Our trials have shown that with the present system the maximum rotation speed is around 1500rpm. There are a number of other factors that can also limit the spinning speed including; vibration in the spinning system, concentricity of the preform to the spinning axis, slight asymmetries in the preform cross-section, slight bends in the preform, alignment of the preform axis to the draw tower axis and purge gas currents in the fiber drawing furnace. All of these must be taken into account when designing and constructing a preform spinning system for the fabrication of short pitch helical-core fibers.

Helical core fibers can be fabricated as single-clad or double clad fibers depending on the refractive index of the coating material applied to the fiber during drawing. For double-clad fibers, a relatively low refractive index (n=1.375) UV cured polymer coating was used resulting in a calculated numerical aperture for the inner-cladding pump guide of ~0.49. In practice, the numerical aperture achieved depends on the curing conditions and is usually a little lower (~0.4) than the calculated value. During the course of this research program we fabricated both passive and active helical-core fibers. The former had a germano-silicate core, fabricated via modified chemical vapour deposition (MCVD), and were used for preliminary experimental studies on the properties of helical-core fibers. The active fibers had Yb-doped alumino-silicate cores and were fabricated via MCVD and solution doping. One problem that we encountered in the early stages of the project with the latter fibers was a large dip in the refractive index profile at the centre of the core (a typical example of which is shown in figure 4(a)). The dip in the index profile was especially pronounced in large core fibers and would clearly have a detrimental effect of beam

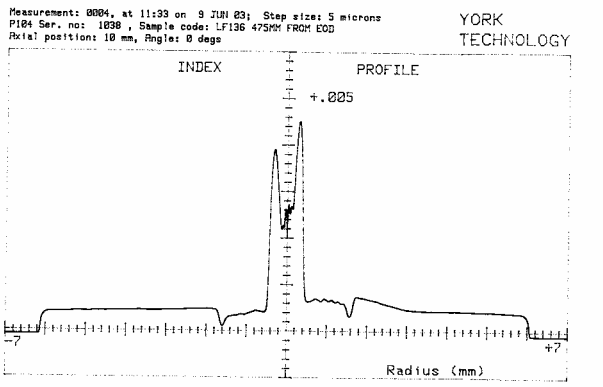


Figure 4(a): Typical refractive index profile of a Yb-doped alumino-silicate core fabricated in the early stages of the project.

quality. For this reason a great deal of effort was directed towards solving this problem to achieve the desired 'top hat' –like index profile. It was found that by careful control of the temperature during the consolidation and collapsing stages proved to be a very effective remedy. An example of a typical refractive index profile for an Yb-doped alumino-silicate core fabricated using the improved fabrication procedure is shown in figure 4(b).

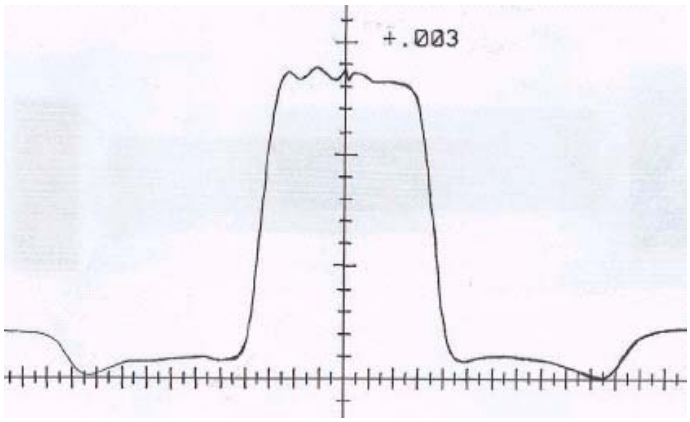


Figure 4(b): Typical refractive index profile of a Yb-doped alumino-silicate core fabricated using the improved procedure.

## 4.0 Characterization of helical core fibers

### 4.1 Core propagation loss and circular birefringence

The first helical-core fiber that we produced had a Ge-doped core fiber and was fabricated by spinning an offset-core preform at a rotational speed of 500rpm and drawing at a pulling speed of 0.9m/min, yielding a pitch of 1.8mm. The resulting fiber had a core of radius of 7μm and 0.14NA with the core offset from the fiber axis by 75μm and had an outer-diameter ≈250μm. The fiber was coated with high-index polymer to facilitate launching of the probe light into the core and characterization of the fiber.

A preliminary investigation of the properties of helical-core fibers was conducted using the simple experimental arrangement shown in figure 5 with the aid of a probe beam provided by a diode-pumped Nd:YAG laser. This laser produced a linearly-polarised, $TEM_{oo}$ beam with $M^2<1.05$ up to a power level of 0.6W. The fiber was cleaved with end facets perpendicular to the fiber axis and the probe beam was launched into the fiber core using standard optics (in this case a 400mm focal length plano-convex collimating lens followed by a 12mm focal length multi-element focusing lens (Newport, F-L10B). This focusing arrangement was initially tested on a standard telecom fiber of core radius 4.3μm and 0.12NA with the result that 80-85% of the incident probe light could be launched. In the case of a helical-core fiber care must be taken to choose the correct orientation of the fiber (i.e. with the core in the uppermost or lowermost positions as shown in figure 6) and with the correct angle of incidence on the facet (i.e. $\theta_i=\text{arc}[n_{co}\sin(\theta_p)]$, where $\theta_p\approx 2\pi Q/P$ is the pitch angle between the core axis and the z direction, $n_{co}$ is the refractive index of the core and Q and P are the core offset and pitch respectively). For

our test fiber, $\theta_i$ was ~22˚ and hence was somewhat larger than arcsin(NA), so launching the probe light at normal incidence would result in a very poor in-coupling efficiency.

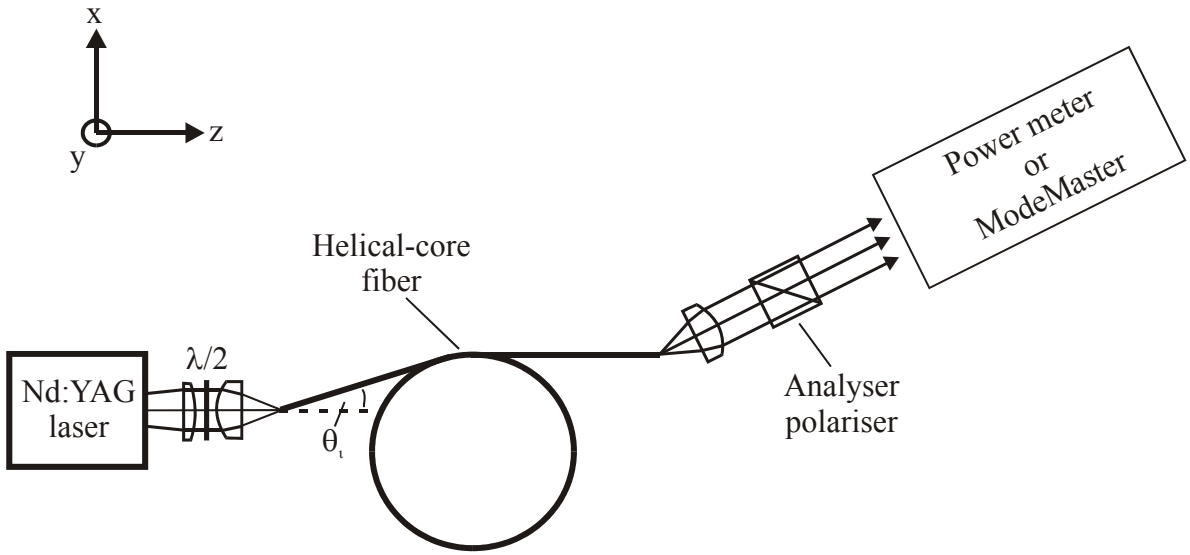


Figure 5 Experimental set-up for investigating the properties of helical-core fibers

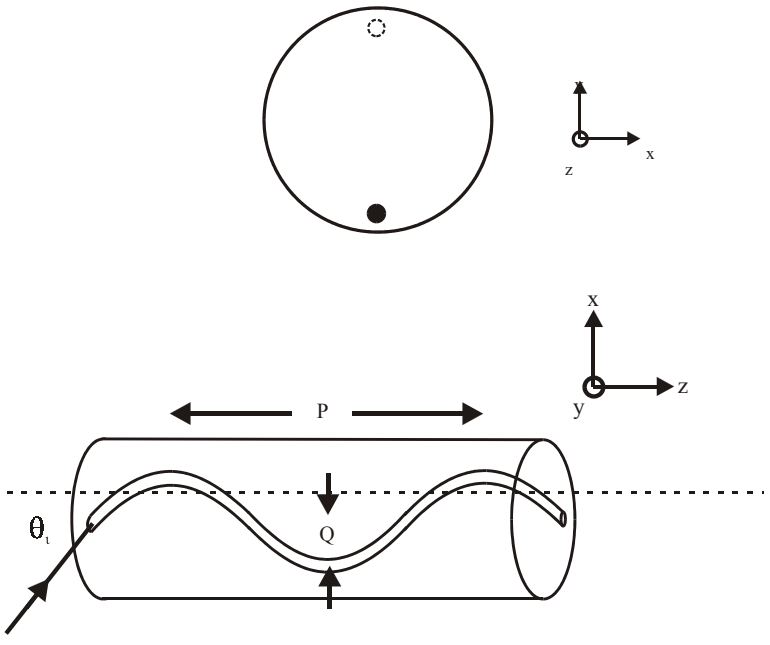


Figure 6: Fiber orientation for efficient launching of probe light

The circular birefringence $\Delta n_{LR}=\left|n_L-n_R\right|$ can be calculated from [4]

$$\Delta n_{LR}=\frac{2\lambda}{P}\left(1-\frac{P}{S}\right) \tag{1}$$

where $S=(4\pi^2Q^2+P^2)^{1/2}$ is the helical length per pitch. For our test fiber, $\Delta n_{LR}=3.85\times10^{-5}$ at the probe beam wavelength of 1.064μm. If the circular birefringence is large enough (i.e. so that it dominates over the effect of any residual linear birefringence), then the polarisation of a linearly-polarised incident beam will be preserved on propagating through the fiber, but with the plane of polarisation rotated by

$$\phi=\frac{\pi L_f \Delta n_{LR}}{\lambda} \tag{2}$$

where $L_f$ is the fiber length. It is worth noting that φ is independent of wavelength since $\Delta n_{LR}\propto\lambda$. By measuring the maximum and minimum power transmitted as the analyser polariser was rotated, we were able to confirm that the fiber maintains the linear polarisation of the probe beam with $P_{max}/P_{min}>60$ and with very little dependence on the plane of polarisation of the incident beam. This result implies that circular birefringence dominates over any residual linear birefringence in this fiber. The circular birefringence was also determined experimentally (using the set-up in figure 5) by cutting back the fiber and measuring the change in polarisation rotation angle φ versus change in fiber length. The results of these measurements (shown in figure 7) suggest that $\Delta n_{LR}=4.1\times10^{-5}$, which is in good agreement with the calculated value for $\Delta n_{LR}$.

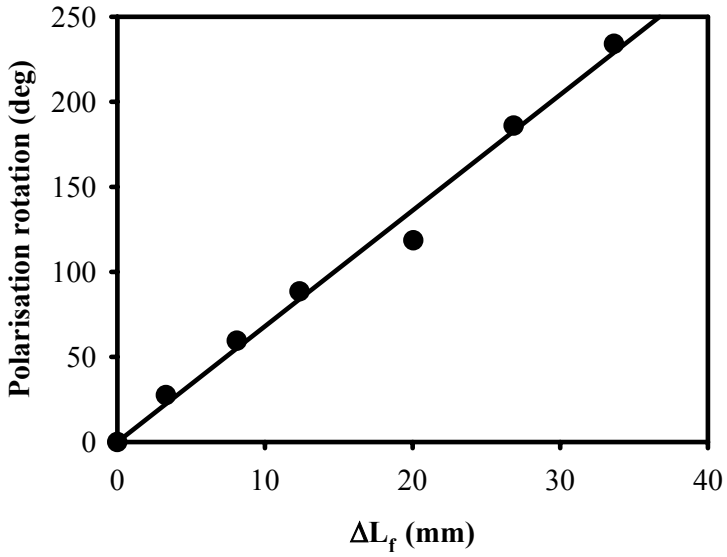


Figure 7: Change in polarisation rotation versus change in fiber length

In addition to polarisation control, another important aim of the project was to see if large core sizes could be used whilst maintaining single-mode operation, preferably with low propagation losses. The rationale behind this idea is that higher-order modes will experience a greater loss, due to the helical-core geometry, and hence will be suppressed. Our test fiber had a relatively large core diameter of 14μm and a normalised frequency parameter, V, of 5.8 at the probe beam wavelength, and so could support propagation of a number of higher order modes. Using the set-up shown in figure 5, we made measurements of the far-field transverse intensity profiles and the beam propagation factor for the output beam from the test fiber. Figure 8 shows a typical far-field beam profile in the y-z plane. The output beam from the fiber is slightly astigmatic with $w_x/w_y \approx 0.94$ in the far-field due to the probe beam exiting the fiber at a non-normal angle of incidence. The far-field beam divergence angles in the x-z and y-z planes are 0.095 and 0.099 radians respectively. The beam propagation factors, $M_x^2$ and $M_y^2$, (in the x-z and y-z planes) were measured using a Coherent ModeMaster to be less than 1.04, indicating that the output beam was single mode.

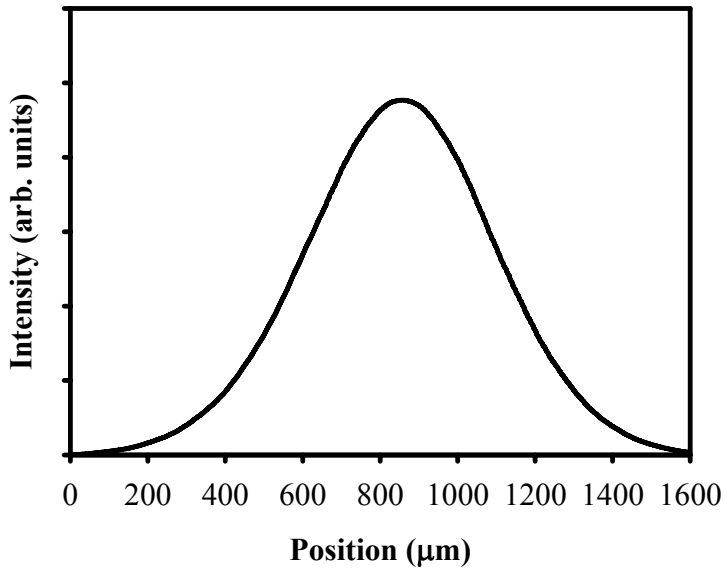


Figure 8: Far-field intensity profile for the output beam in the y-z plane.

The core propagation losses were determined by cutting back the fiber and measuring the fraction of the incident power transmitted. The results (shown in figure 9) indicate that the launch efficiency with respect to incident power is ~70% and the core propagation loss for the fundamental mode is ~1.5dB/m.

Device lengths in high-power cladding-pumped fiber lasers and amplifiers are typically in the range of a few metres to a few tens-of-metres (depending on the rare earth ion concentration and inner-cladding-to-core area ratio), so the loss for this test fiber is a little too high for a practical device. However, the results for this fiber were quite encouraging since they indicate that there

is scope for a reduction in propagation loss (e.g. by increasing the pitch), whilst still retaining the desirable properties of helical-core fibers (i.e. polarisation preservation and suppression of higher-order modes).

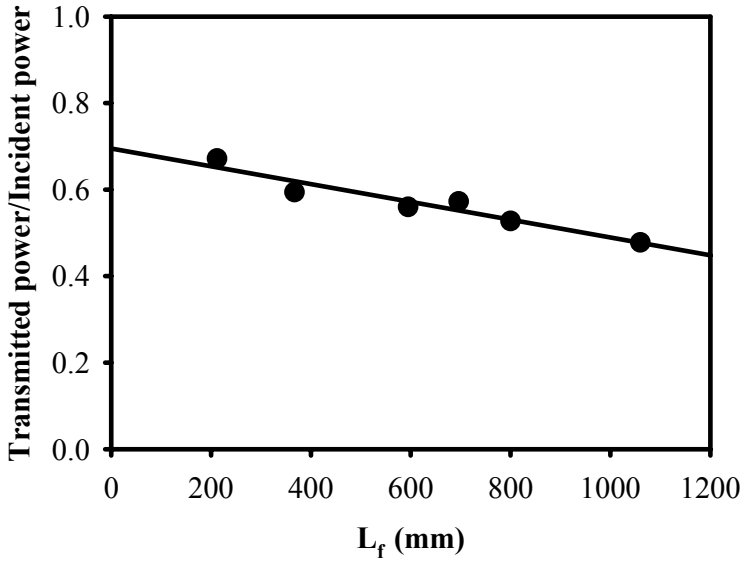


Figure 9 Transmitted power versus fiber length

In order to confirm this we conducted further studies on helical-core fibers with a range of different pitches and core offsets. The following fibers were fabricated and characterized at 1.064μm using the procedure described above.

| Fiber | Inner-cladding diameter (μm) | Core offset (μm) | Pitch (mm) | Radius of curvature (mm) | Loss (dB/m) | $\Delta n_{LR}$ |
|---|---|---|---|---|---|---|
| A | 380 | 133 | 4.0 | 3.05 | 1.0 | $1.08\times10^{-5}$ |
| B | 400 | 130 | 3.9 | 2.96 | 1.2 | $1.16\times10^{-5}$ |
| C | 400 | 115 | 4.0 | 3.52 | 0.46 | $0.85\times10^{-5}$ |
| D | 400 | 115 | 3.9 | 3.35 | <0.1 | $0.91\times10^{-5}$ |
| E | 400 | 115 | 3.8 | 3.18 | - | $0.99\times10^{-5}$ |
| F | 400 | 115 | 3.7 | 3.02 | - | $1.07\times10^{-5}$ |

Table 1: Helical-core fiber parameters

All fibers of the fibers used in this study had the same core diameter (~26μm) and core NA (0.14), and hence a V-value of 10.7 at the probe beam wavelength of 1.064μm. The measured propagation loss for the fundamental mode for fibers A, B and D decreases with increasing radius of curvature as expected. Our measurements indicate that the propagation loss decreases very rapidly with increasing radius of curvature, implying that very precise selection and control of the pitch is needed (i.e. <2%) to obtain a helical-core fiber with the desired characteristics.

The results for fiber C appear, at first sight, to be inconsistent with expectations. However, only a limited length of this fiber (~3.5m) was available with the result that when the fiber was cut-back to determine propagation loss the output beam quality degraded. We believe this is due to the propagation loss being too low to completely suppress higher-order modes in the short length of fiber. The net result is that the measured propagation loss includes a contribution for higher order modes, and hence is somewhat higher than would be expected. It should be noted that for the lengths of fiber used in the determination of propagation loss for fibers A, B and D, the output was single mode. We were unable to determine the losses for fibers E and F because the transmitted power varied markedly depending on how the fibers were arranged. In fact, even applying light pressure to the fiber (e.g. by pressing it down on to the optical table) resulted in a significant change in transmitted power, and hence loss. This could be due to breaks in the fiber suggesting that there may be a problem in the fabrication procedure for short pitch fibers. Further investigation is needed to confirm this. Fibers A, B, C and D did not exhibit this behaviour.

Fiber D had a measured loss for the fundamental mode of <0.1dB/m and the transmitted probe beam was single-mode ($M^2 \approx 1.1$) for fiber lengths >4.5m. In addition, the circular birefringence ($\Delta n_{LR}=0.91\times10^{-5}$) was high enough to maintain the linear polarization state of the probe beam with $P_{max}/P_{min}>40$. This is a very encouraging result, since the propagation loss is low enough for a practical device. Clearly, further experiments on undoped helical-core fibers will be needed to determine the dependence of propagation loss on core NA, core size and wavelength to obtain an estimate of the upper-limit on core size that can be used. However, the experimental data obtained from these preliminary experiments was considered to be sufficient for a first attempt at a design for an Yb-doped helical-core fiber laser.

### 4.2 Pump propagation loss in double-clad helical core fibers

An ytterbium-doped helical core fiber with inner-cladding diameter of 400µm, core diameter of 25µm (NA=0.14), core-offset of 115µm, pitch of 3.9mm and Yb concentration of 2500ppm was fabricated. The design was identical to that of fiber D (discussed in section 3.3.1) except that the fiber was coated with a low refractive index polymer (UVF375) for cladding pumping. This design was expected to have a core propagation loss for the fundamental mode of <0.1dB/m at 1-1.1µm, but a direct measurement of the propagation loss in this wavelength regime would be difficult due to the Yb absorption.

A simple experiment to determine the pump absorption efficiency in the Yb-doped helical-core fiber was performed. For these experiments, the output beam from a high-power diode pump source at 940nm was coupled into the fiber's inner-cladding with a launch efficiency of >80%. The launch efficiency was determined by replacing the helical-core fiber with a core-less fiber with approximately the same inner-cladding size. When the core-less fiber was replaced by a ~30-40cm length of the Yb-doped helical-core fiber and the launch efficiency optimised only just over 20% of the incident pump light was transmitted indicating that the pump propagation losses are extremely high. This could not be explained by Yb absorption, since, based on the cladding-to-core area ratio and Yb concentration, we would normally require several tens-of-metres of fiber for efficient pump absorption. To check this we replaced the Yb-doped fiber by 1m of

undoped helical-core fiber with a similar inner-cladding diameter (~400μm) and the same low refractive index outer-cladding. We estimated the pump propagation loss to be ~6dB/m. This is a little lower than the loss for the Yb-doped fiber, but still far too high for a practical device. There are a number of possible mechanisms which may contribute to this loss as follows: (a) Internal scattering/absorption in the inner-cladding, (b) Scattering at the inner-cladding/outer-cladding interface and (c) Reflection from the core-cladding interface. The undoped and Yb-doped helical-core fiber preforms were both made using the 'stacked-rod' approach. If the rods were not properly cleaned prior to collapsing, or if some air remained trapped then this could result in absorption/scattering of the pump light. A further problem is that the collapsed preform did not have a perfectly circular cross-section, so that when the preform is spun, the inner-cladding of the fiber has a twisted 'rope-like' appearance. This may result in scattering from the inner-cladding/outer-cladding interface. It was interesting to note that inner-cladding of the undoped fiber was much smoother than the doped fiber and had a lower pump propagation loss. This seemed to indicate that the surface quality of the inner-cladding is an important factor.

To allow further investigation of the origin of the pump propagation loss, we fabricated double-clad Yb-doped helical-core fibers with a core-offset of 143μm and pitches of 4.0 and 7.6mm, corresponding to equivalent bend radii of 3 and 10mm respectively. For comparison, we also fabricated a double-clad straight-core fiber from the same preform. All fibers had the same core and inner-cladding diameters of 27μm and 440μm respectively, and a core NA of ≈0.14.

The background inner-cladding propagation loss was measured by the "cut back" method. A white light source was used to launch broadband light into the inner-cladding at one end of the fiber and the output spectrum of light emerging from the opposite end was recorded by an optical spectrum analyzer (OSA). By comparing the absorption spectra for different lengths of fiber, the Yb absorption coefficient and background loss could be determined. An example of a typical absorption spectrum for the 7.6mm pitch helical-core fiber is shown in figure 10 and the results for all three fibers are summarized in Table 2.

| Inner-cladding diameter (μm) | Pitch (mm) | Core offset (μm) | Radius of curvature (mm) | Background loss (dB/m) |
|---|---|---|---|---|
| 400 | 4 | 143 | 3 | 1 |
| 440 | 7.6 | 143 | 10 | 0.24 |
| 440 | Straight-core | 143 | ∞ | 0.08 |

Table 2: Background inner-cladding loss for 4mm and 7.6mm pitch and straight-core fibers.

The results appear to confirm that the higher background (inner-cladding) propagation loss is associated with the helical-core geometry. The loss decreases as the pitch (i.e. radius of curvature) is increased. The most likely origin of this increased loss is reflection from the core-inner-cladding interface (as illustrated in figure11). For efficient cladding-pumping, the background inner-cladding loss must be much lower than the pump loss due to Yb absorption. The latter depends on the inner-cladding-to-core area ratio, Yb concentration and the pump

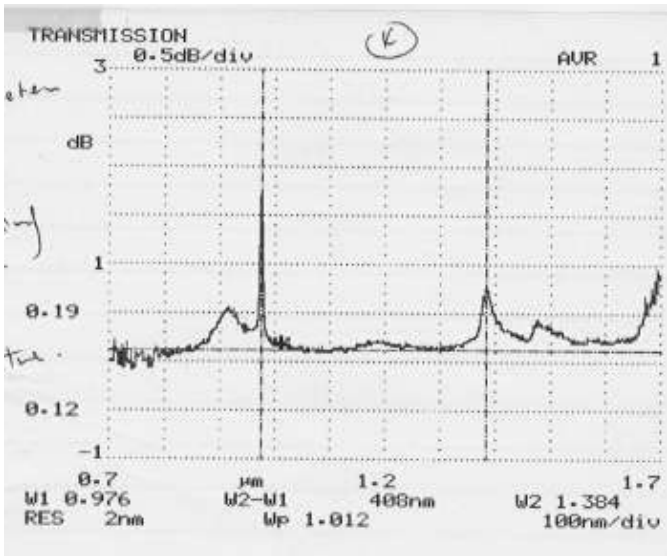


Figure 10: Absorption spectrum for 7.6mm pitch helical-core fiber

wavelength. For this fiber design the Yb absorption coefficient is ~0.5dB/m at 940nm, implying that a background loss for the pump of <0.1dB/m is needed for efficient operation. The background loss can be reduced by using a longer pitch and/or smaller core-offset, and by reducing the core NA. This strategy has proved to be very effective in realizing efficient single-mode operation in a cladding-pumped helical-core laser as will be discussed later. However, there is one major disadvantage which is that it is difficult (perhaps impossible) to achieved the required level of circular birefringence for polarisation maintenance whilst at the same time having a low enough background inner-cladding loss for efficient cladding pumping. A more detailed numerical study of the inner-cladding loss versus absorption efficiency has been conducted by Dr Gerry Moore at Kirtland AFB. The preliminary findings of this study appear to be in reasonable agreement with our experimental measurements for inner-cladding loss.

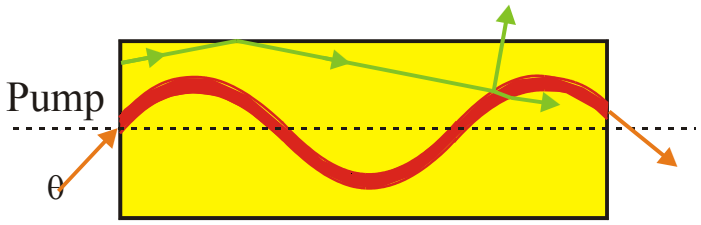


Figure 11: Origin of inner-cladding background loss

## 5.0 Diode-stack pump module and coupling scheme

Prior to the date this project commenced, cladding-pumped fiber lasers and amplifiers generally employed pump sources (e.g. fiber-coupled broad-area diodes and fiber-bundle-coupled diode-bars) of moderate power up to several tens-of-watts. Scaling such systems to higher power requires quite complicated (and expensive) pump multiplexing schemes. We therefore decided to investigate an alternative approach for power-scaling based on the use of diode-stacks. The rationale for this approach was that diode-stacks offer the highest output power of any commercially available diode (and are also the cheapest per watt). The net result is that fewer pump diodes and fewer optical components are required in the pump launching scheme thus reducing the overall complexity and cost. The main disadvantage of diode-stacks is the poor quality and unfriendly nature of their output beams. The beam propagation factor parallel to the diode array, $M_x^2$, is typically ~2000, and is many times larger than the beam propagation factor, $M_y^2$ (after fast axis collimation), in the stacking direction, making it difficult to focus to the small beam sizes required for efficient cladding pumping.

One solution to this problem is to re-shape the output beam so that $M_x^2 \approx M_y^2$, but without significantly degrading the brightness. The approach that we explored in the early stages of the project was based on the use of a two-mirror beam-shaper [5].

### 5.1 Beam-shaped diode-stack pump module

The two-mirror beam shaping technique was developed in-house at the ORC several years ago and has been successfully applied to broad-area diodes and diode-bars to allow efficient end-pumping of solid-state lasers and low-medium power double-clad fiber lasers. The principle of operation of the two-mirror beam-shaper is described in detail in ref. 5. The basic idea (shown schematically in figure 12) is to use two high reflectivity mirrors to slice-up the combined output beam from the diode source in the x direction and stack the resulting beams in the orthogonal direction. As a rough guide, we can achieve a reduction in the value for $M_x^2$ to $M_x^2/N$ and an increase in the value for $M_y^2$ to $NM_y^2$, where N is the number of times the incident beam is sliced. N is normally selected (e.g. by adjusting the mirror separation and/or orientation, and/or the incident beam size) so that the emerging beam has roughly equal $M^2$ values in orthogonal planes. In practice, there is a small reduction in brightness due to leakage through the mirrors and because $M_y^2$ after beam shaping is $>NM_y^2$, since it is necessary to separate the stacked beams in the y-direction by a greater distance than the incident beam height to avoid loss due to clipping at the entrance aperture of the beam shaper. Further reduction in brightness can be avoided, or minimized, by careful design and alignment of the beam shaper, and careful selection of the incident beam dimensions. The key attractions of this approach are low loss and simplicity, since only two relatively standard components (i.e. mirrors) are required for beam shaping. Obviously, further complexity is added due to the need for a combination of cylindrical and spherical lenses for conditioning of the output beam from the diode laser to match the requirements for beam shaping and, also, for re-collimating and focusing of the re-shaped output beam.

We have applied this approach to a 480W cw (12-bar) diode-stack operating at ~938nm (purchased from DILAS DiodenLaser GmbH) using the optical arrangement shown in figure 13. The output from each bar on the stack was first collimated by a high numerical aperture cylindrical microlens (FAC-850 from LIMO GmbH), and then imaged on to the entrance aperture of the two mirror beam-shaper via an arrangement of crossed cylindrical lenses, $f_1$ and $f_3$, and $f_2$ and $f_4$ respectively. The lenses were selected to produce a highly elliptical beam with $w_x >> w_y$,, where $w_x$ and $w_y$ are the beam widths in the x and y directions respectively. It is important that the beam width in the y direction is not too small, so that the Rayleigh range, $z_{oy} > w_x$, otherwise there is significant diffraction spreading of the beams in the y-direction as they pass through the beam shaper, leading to a reduction in brightness. Based on the diode-stack specifications available from the manufacturer we estimate that initial beam propagation factors (i.e. before beam shaping) would be $M_x^2 \sim 2000$ and $M_y^2 \sim 45$ (after collimation by the microlens array). The latter value takes into account the likelihood that there will be some degradation in the beam quality for each diode-bar during collimation due to lens aberrations and misalignment. It should be stressed that accurate alignment of the microlenses is crucial for good performance of the whole focusing system. Our aim was to configure the beam shaper to produce a re-shaped beam with beam quality factors in orthogonal planes $M_{xf}^2 \approx M_{yf}^2 \approx (1.3 M_x^2 M_y^2)^{1/2} = 340$ by slicing the input beam ~6 times. The factor of 1.3 is to allow for extra spacing between stacked beams in the y direction to minimize loss due to clipping on the first beam-shaper mirror. To achieve this, focal lengths, $f_1$=38mm, $f_2$=200mm, $f_3$=150mm and $f_4$=50mm, were selected to produce a beam of width ~40mm in the x direction and ~4mm in the y-direction at the beam-shaper entrance aperture. We obtained 480W of output power from the beam shaper at the maximum drive current, which corresponds to 520W after collimation by the microlenses. This is a much higher transmission than is usually achieve with single bars or broad-area diodes due to the 'top-hat' intensity profile of the beam in the y direction.

The output from the beam-shaper was re-collimated in the x direction by a cylindrical lens of focal length 300mm and then focussed by a Gradium lens of focal length 25mm. At the waist we measured beam radii of 380μm and 490μm in the x and y directions respectively. The values for $M_{xf}^2$ and $M_{yf}^2$ were determined using a scanning slit to measure the beam size versus position. We found that $M_{xf}^2 \approx 305$ and hence was somewhat smaller than expected. Unfortunately, $M_{yf}^2$ was much larger than expected with a value of approximately 790. This was attributed mainly to inaccurate positioning of the fast-axis collimating lenses in the y and z directions (see figure 13). The tolerance for positioning of these lenses relative to each other in the y direction, so that collimated beams propagate parallel to each other, is very tight and difficult to meet. As a very rough guide, the degradation in beam quality for the combined beam in the y direction will become significant when the angular misalignment, $\Delta\alpha$, of collimated beams from adjacent bars is comparable to the beam divergence, $\theta_B$ of an individual collimated beam. To avoid degradation beam quality requires $\Delta\alpha << \theta_B$, which in turn requires that the tolerance on positioning of the microlenses in the y direction for adjacent bars, $\Delta y << h_e$, where $h_e$ is the beam size in the y direction at the diode-bar facet (typically ~1μm).

To improve the final beam quality, we refined our procedures for aligning and fixing the microlenses in position. We are now able to position adjacent microlenses in the y direction to an accuracy of around ±0.5μm. There is still scope for further improvement, but this is probably the best that we can achieve for the time being. Further improvements in microlens positioning

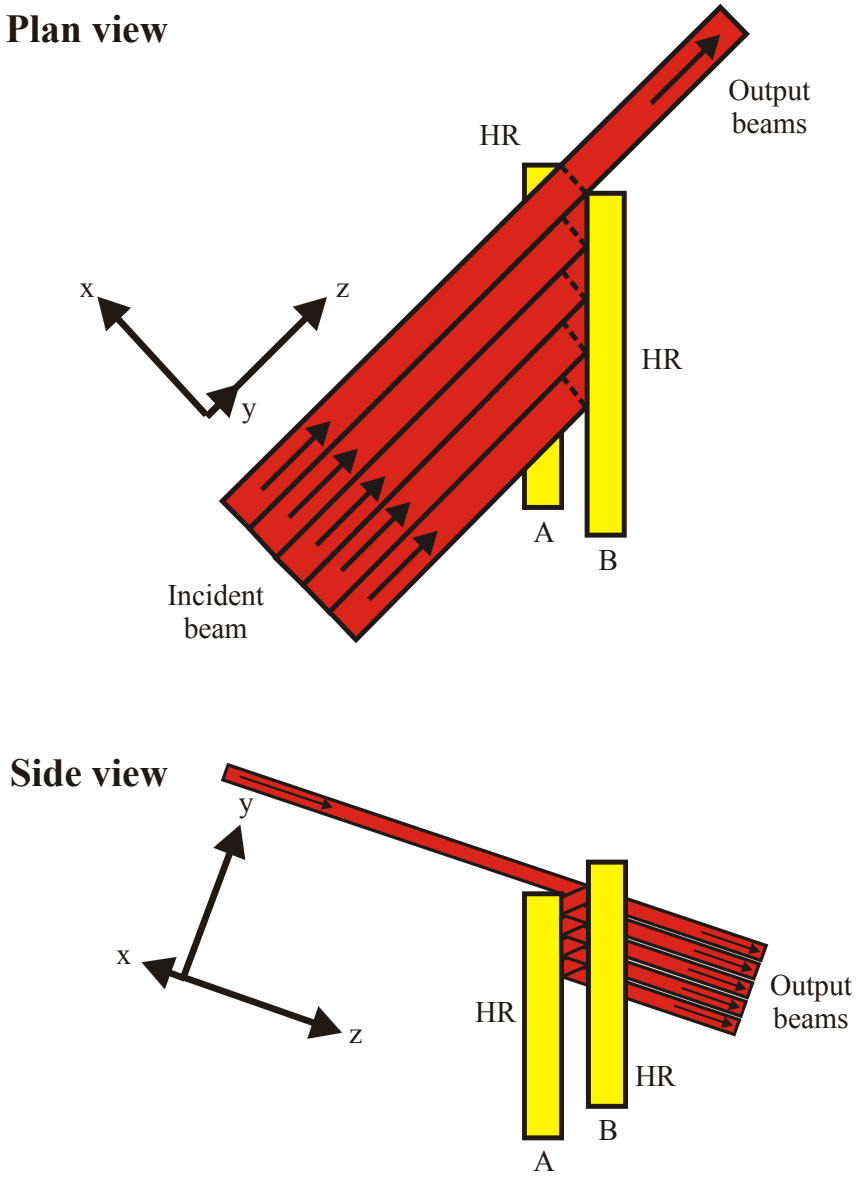


Figure 12. Two-mirror beam-shaper

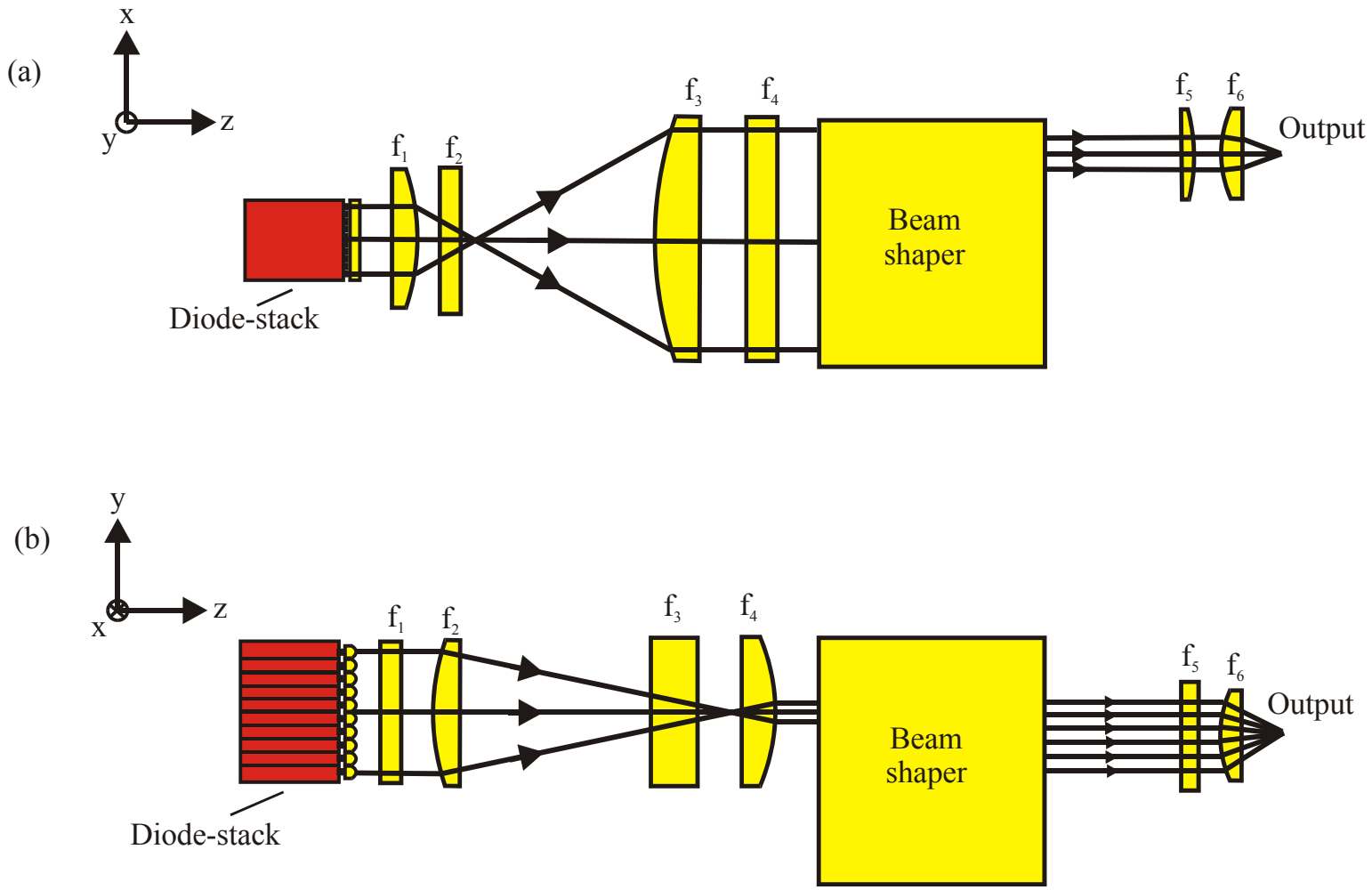


Figure 13: (a) Plan view and (b) side view of diode-stack focusing scheme

may, in any case, be offset by other sources of degradation in beam quality in the y direction (e.g. diode-array curvature ('smile'), and microlens quality).

The beam-shaped 480W cw (12-bar) diode-stack pump module was re-assembled using the new microlens alignment procedure and tested. For the new set-up we obtained beam quality factors, $M_{xf}^2 \approx 335$ and $M_{yf}^2 \approx 340$, in the x and y directions respectively. A photograph of the beam-shaped diode-stack pump module is shown in figure 14. The minimum inner-cladding diameter, required for efficient launching of the output from the pump module can be estimated from:

$$d = \frac{2\gamma_w \gamma_{na} M^2 \lambda_p}{\pi \theta_{na}} \tag{3}$$

where $\theta_{na}$=arcsin(NA), and $\gamma_w$ and $\gamma_{na}$ are the ratios by which the focussed beam size and far-field beam divergence should under fill the fiber inner-cladding diameter and $\theta_{na}$ for efficient in-

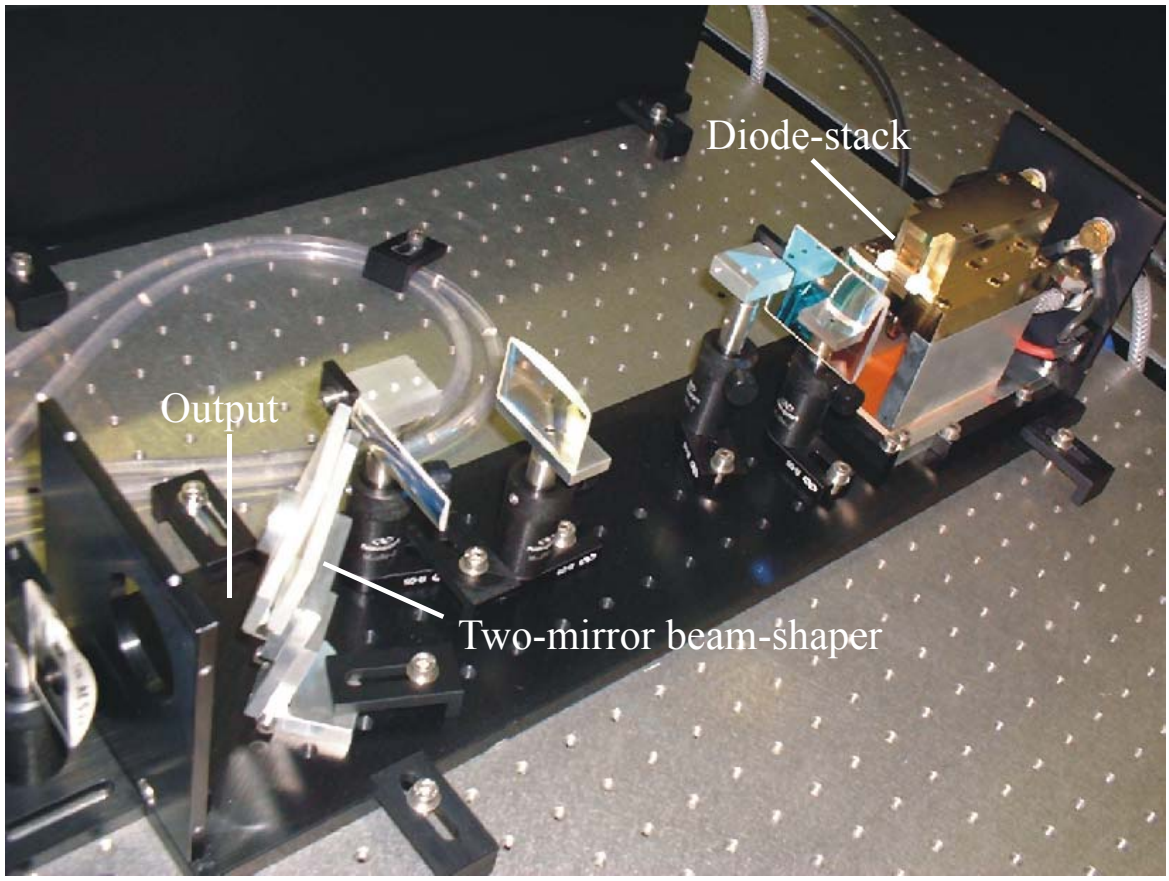


Figure 14: Beam-shaped diode-stack pump module

coupling respectively. The values of $\gamma_w$ and $\gamma_{na}$ need to be selected to give a high launch efficiency, but without resulting in a significant degradation in the beam quality on launching into the fiber. If we choose $\gamma_w \approx \gamma_{na} \approx 1.2$ (to achieve high launch efficiency and minimise the risk of damage caused by un-coupled pump light), and the inner-cladding NA is 0.4, then the minimum inner-cladding dimensions required diameter required are ~ 500μm for the x and y direction respectively. There is certainly scope for a further improvement in the output beam quality and hence brightness from the beam-shaped diode-stack, allowing coupling into smaller diameter fibers, by improving the positioning accuracy of the fast-axis collimating lenses.

## 5.2 Spatially-combined two-stack pump module

For some of the final fiber laser experiments performed in the project use was made of pump module developed in another project. This pump module comprised two 480W diode-stacks at 976nm. The beam divergence of the constituent bars was reduced in orthogonal planes using fast-axis collimating lenses and slow-axis lens arrays, and the resulting beams from the two stacks were spatially-combined by inter-leaving the beams using a slotted-mirror beam-combiner. The resulting combined beam was then split into two beams in the slow directions, which were then re-combined using a polariser and half-wave plate (as shown in figure 15) to produce a single beam with $M_x^2 \approx 200$ and $M_y^2 \approx 150$. The maximum power available after spatial and polarisation multiplexing was ~750W.

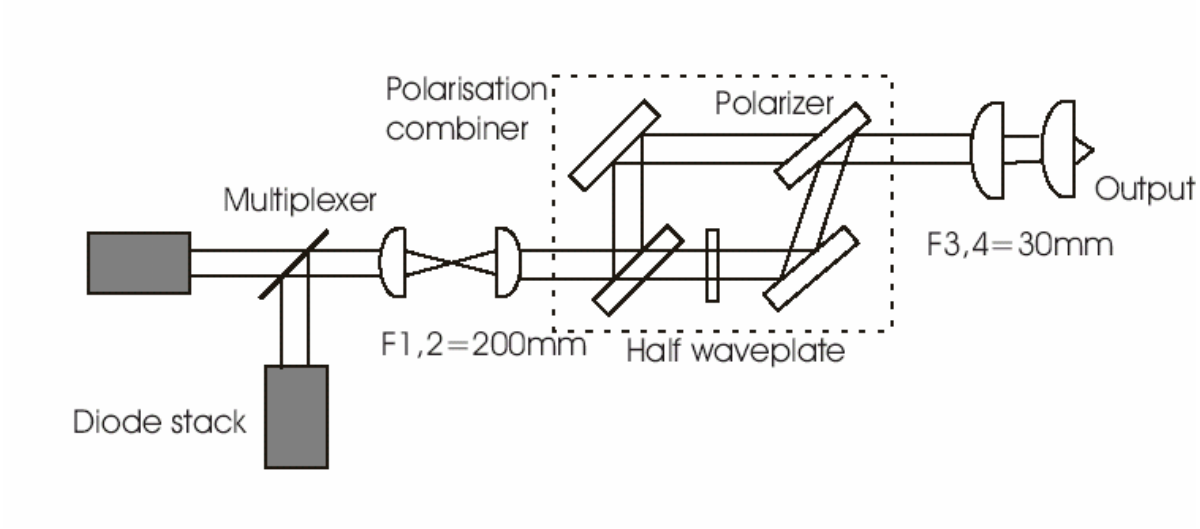


Figure 15: Two-stack pump module at 976nm.

## 6.0 Core-pumped Yb-doped helical core fiber laser

Prior to performing a detailed investigation on cladding-pumped helical-core fiber laser and amplifiers, we conducted a study on core pumping of Yb-doped helical-core fiber lasers (YHFL's) to see if efficient linearly-polarised, single-mode operation could be achieved in a large-core laser device.

The experimental arrangement used for core pumping the YHFL is shown in figure 16. For convenience we decided to use an Yb:YAG laser (constructed in-house) as the pump laser. The Yb:YAG laser employed a simple cavity design comprising a plane pump input mirror with high

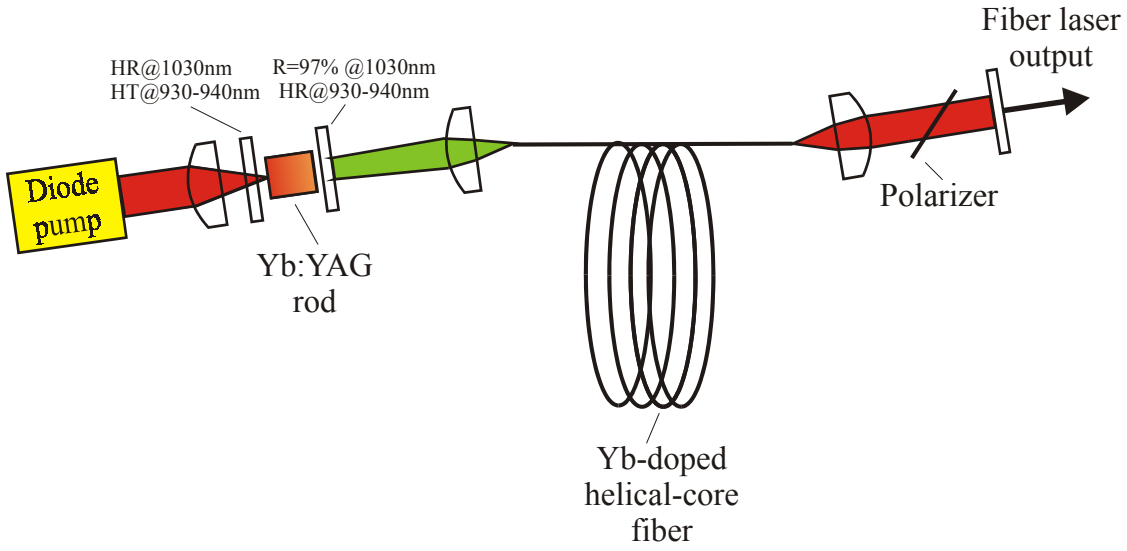


Figure 16. Core-pumped Yb-doped helical-core fiber laser

reflectivity (>99.8%) at 1030nm and with high transmission (>90%) at 940nm, a 3mm long YAG rod doped with 5at.% $Yb^{3+}$ and a plane output coupler with reflectivity ~97% at 1030nm. The Yb:YAG rod was end-pumped by the focused output from a beam-shaped diode-stack with thermal lensing in the Yb:YAG providing the means generating stable resonator modes. Due to the relatively low pump absorption efficiency (~30%) for a single-pass of the Yb:YAG rod, an output coupler with high reflectivity at the pump wavelength was used to improve the pump absorption efficiency by double passing the pump. Even with this arrangement, a significant fraction of the pump is fed back to the diode, so the maximum incident pump power was limited to ~55W to reduce the risk of damage. At the maximum pump power we obtained 10W of output from the Yb:YAG laser at 1030nm in a beam with $M^2 \approx 4.4$. The output power and beam quality factor as a function of incident pump power are shown in figure 17.

The YHFL design employed two external cavity arrangements at both fiber ends to provide feedback for lasing. At the pump in-coupling end, feedback for lasing was provided by the combined effect of the pump focusing lens and the Yb:YAG laser output coupler, thus avoiding

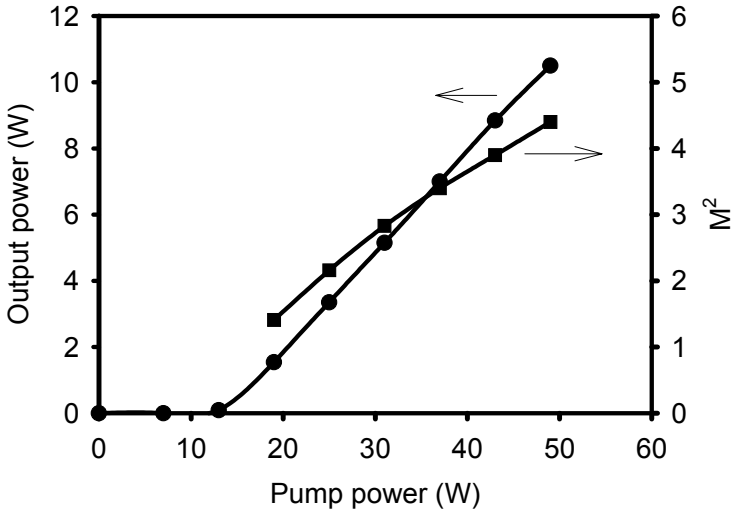


Figure 17: Yb:YAG laser output power and beam quality factor versus pump power

the need for mirrors with expensive dielectric coatings. At the opposite fiber end, feedback for lasing was provided by an external cavity comprising a collimating lens and 20% reflectivity plane output coupler. A thin film polariser was placed between the collimating lens and output coupler to select a linearly-polarised mode. From figure 18 it can be seen that the core absorption coefficient at 1030nm for an Yb concentration of 10,000 ppm is ~21dB/m, indicating

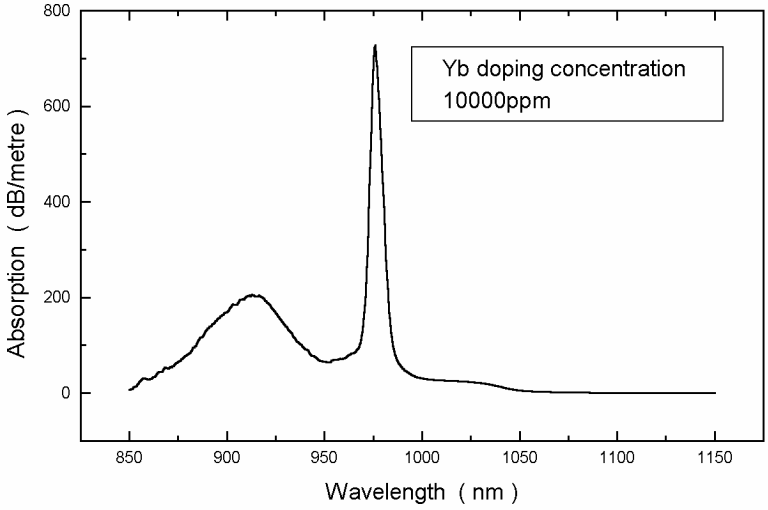


Figure 18: Absorption spectrum for Yb-doped alumino-silicate core fiber

that a fiber length >0.5m would be required for efficient pump absorption. The fiber end facets were cleaved perpendicular to the fiber axis, so that light from the core emerges from the fiber at an angle $\theta_i$ to the fiber axis given by $\theta_i=\arcsin[n_{co}\sin(\theta_p)]$, where $\theta_p\approx 2\pi Q/P$ is the pitch angle between the core axis and the z direction, $n_{co}$ is the refractive index of the core and Q and P are the core offset and pitch respectively. This helps to suppress parasitic lasing due to broadband feedback between the fiber end facets. However, with this arrangement it is important that the fiber is aligned correctly with respect to the pump beam and the external cavities to ensure efficient launch of pump light from the Yb:YAG laser and for efficient feedback of the YHF output from the external mirrors into the core.

With the above experimental set-up and a 1.5m length of standard (straight-core) Yb-doped fiber with a core diameter of 15µm and 0.14NA we obtained a maximum output power of 4W at 1049nm for ~10W of incident pump power. The overall efficiency was limited by a relatively low pump launch efficiency due to the poor beam quality of the Yb:YAG laser. Unfortunately, we were unable to achieve lasing for the YHF described in section 3.3.2 in the same set-up, suggesting that the core propagation losses were much higher than expected based on our previous measurement of core propagation loss for an undoped helical-core fiber with the same design. Further investigation has revealed that the NA for the Yb-doped fiber was somewhat lower than for the undoped fiber, hence explaining the higher helical loss. Our current method for determining the effective NA of the core is based on an estimate of the refractive index step size $\Delta n$ for the preform from $\Delta n\approx[\int n(r)dr]/d$, where d is an estimate for the effective core diameter. Undoped germano-silicate and Yb-doped alumino-silicate fibers have quite different index profiles, so it is difficult to make an accurate comparison of their NA's using the above method. We therefore fabricated a number of Yb-doped helical-core fibers of similar design to the fiber described above, but with longer pitches in the range 4.0 to 8.0mm. The details of the fibers are summarised in table 3.

| **Fiber** | **Pitch (mm)** | **Core offset (µm)** | **Coating** | **$\Delta n_{LR}$ ($10^{-5}$)** | **Radius of curvature (mm)** |
|---|---|---|---|---|---|
| A | 8.00 | 130 | Low index | 0.137 | 12.5 |
| B | 7.14 | 130 | High index | 0.192 | 9.9 |
| C | 6.67 | 130 | High index | 0.236 | 8.7 |
| D | 6.12 | 130 | High index | 0.305 | 7.3 |
| E | 5.66 | 130 | High index | 0.384 | 6.2 |
| F | 5.17 | 130 | High index | 0.502 | 5.2 |
| G | 4.92 | 130 | High index | 0.582 | 4.7 |
| H | 4.76 | 130 | High index | 0.642 | 4.4 |
| I | 4.55 | 130 | High index | 0.733 | 4.0 |
| J | 4.00 | 130 | Low index | 1.072 | 3.1 |

Table 3: Yb-doped (10,000ppm) helical core fibers

Fibers B, D, F, I and J have been tested using the set-up for core-pumping shown in figure 16. A summary of the results obtained is given in Table 4. Fibers I and J, with the shortest pitches and

| Fiber | Pitch (mm) | Fiber length (m) | Pump power (W) | Threshold Power (W) | Output power (W) | Emission wavelength (nm) | Extinction ratio | $M^2$ |
|---|---|---|---|---|---|---|---|---|
| B | 7.14 | ~8 | 4.6 | - | 1.00 | 1074-1085 | 10 | ~1.8 |
| D | 6.12 | ~4 | ~7.0 | ~1.3 | 0.84 | 1074-1085 | 4 | 1.25 |
| F | 5.17 | ~3 | 2.2 | ~0.5 | 0.39 | 1047 | >10 | 1.1 |
| I | 4.55 | - | - | - | - | - | - | - |
| J | 4.00 | - | - | - | - | - | - | - |

Table 4: Summary of YHFL performance

hence the highest propagation losses, did not lase. However, fibers B, D and F all operated as lasers with relatively good beam quality (i.e. $M^2$<1.8) and operating wavelengths between 1047 and 1085nm depending on the fiber length (see figure 19). Fiber lasers B and D produced single-mode output beams with $M^2$<1.25 (see figure 20). In contrast, an Yb-doped fiber with a straight core of the same diameter and NA (i.e. V=10.7) produced an output beam with $M^2$>5, thus

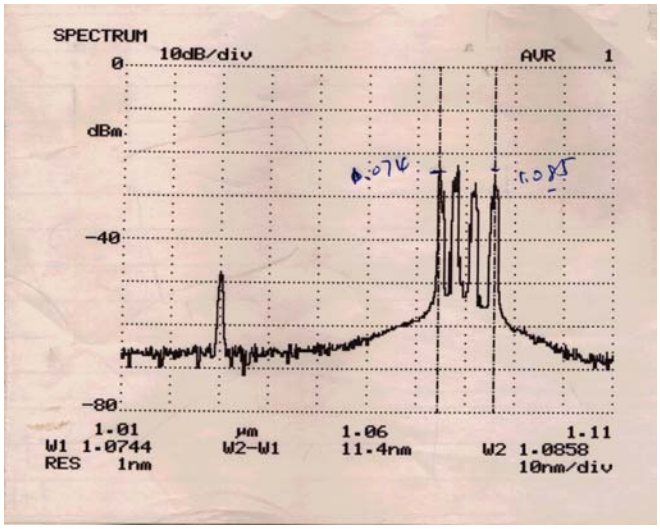


Figure 19: Emission spectrum of fiber laser D

serving to confirm the benefits of the helical geometry. The slope efficiencies with respect to incident power for fibers B, D and F (~ 17-27%) were somewhat lower than one might expect for Yb fiber lasers. We believe that this is mainly due to the higher propagation loss for the multimode pump beam due to the helical geometry. Further optimisation of the fiber design should yield an improvement in the efficiency. Fiber lasers B and F produced a linearly-polarised output with only 10% of the light rejected by the thin film polariser. Fiber laser D did not perform as well as fiber lasers B and F, both with respect to overall efficiency and

polarisation maintenance. The reasons for this are unclear and require further investigation. The extinction ratios (i.e. $P_x/P_y$) for all of the YHFL's are somewhat lower than those achieved in the undoped helical-core fibers, indicating that the circular birefringence may a little lower than is needed for robust polarisation maintenance. Using a shorter pitch fiber, with a higher NA to keep the propagation loss low enough for efficient operation, may help to solve this problem.

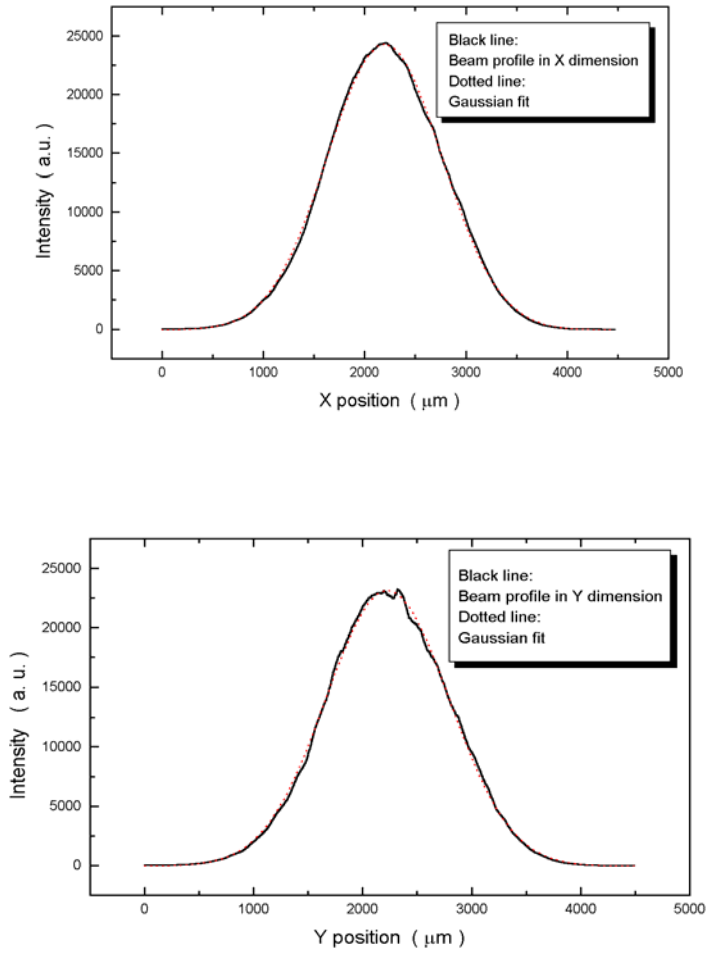


Figure 20: Transverse intensity profile of fiber laser D output in the x and y directions

## 7.0 High power tunable cladding-pumped Yb-doped offset-core fiber laser

Fiber lasers have very broad emission linewidths and hence offer a great deal of flexibility in operating wavelength. The combination of power scalability and wavelength flexibility is almost unique to fiber-based sources and is potentially very useful for a range of applications. In the absence of wavelength selection, cladding-pumped Yb-doped fiber lasers typically operate at relatively long wavelengths ~1090nm due to their long device lengths. From a power scaling point of view operation at shorter wavelengths may be advantageous since the heat loading due to quantum defect heating is reduced. In the case of Yb-doped fiber lasers it should be possible, via the use of an appropriate means for wavelength selection, to reduce the heat loading by up to a factor-of-two. Helical-core fibers may be advantageous in this respect since the 'helical loss' is wavelength dependent and is higher for longer wavelengths. This raises an interesting question which, is namely, what range of operating wavelengths can one achieve in a conventional cladding-pumped Yb-doped fiber laser when operated in a simple tunable laser configuration. We have conducted a simple experimental study on a typical double-clad Yb-doped offset-core fiber. The fiber had a multimode alumino-silicate core of diameter, 26μm and NA, 0.14, doped with Yb at a concentration level of 10,000ppm and a pure silica circular inner-cladding of diameter 440μm. The core was offset from the fiber axis by ~143μm to promote efficient pump absorption and the inner-cladding was coated by low refractive index (n=1.375) polymer outer-cladding to provide a high numerical aperture of 0.49 (calculated) for the pump guide.

The experimental arrangement used for the tunable Yb-doped fiber laser is shown in figure 21. The 12-bar diode-stack pump module at 940nm (described earlier) was used to pump the fiber laser. At the maximum operating current for the diode-stack, the pump power available at the focus was 430W compared with ~480W immediately after the beam-shaper and ~ 515W at the diode-stack. The beam propagation factors, $M_x^2$ and $M_y^2$, after the final focusing lens were measured as 335 and 340, in accordance with expectations. If we assume for efficient launching into a double-clad fiber that the pump beam diameter and far-field beam divergence must underfill the inner-cladding diameter, $D_f$, and $\theta_{NA}$=arcsin(NA) by a factor of 1.2, then as a rough guide we require $M_{x,y}^2 \leq 1.1 D_f \theta_{NA}/\lambda$. Hence, we require a diode source with $M_{x,y}^2 \leq 210$ for efficient coupling of pump light into our fiber. This could be achieved by improving the alignment of the fast-axis cylindrical microlenses and by using a slow-axis lens array to reduce the slow-axis beam divergence. Alternatively, a fiber with a larger diameter inner-cladding could be employed. However, with this pump coupling arrangement and the present fiber design the pump launch efficiency was limited to ~39% at high power levels.

The tunable fiber laser employed an extended cavity comprising an antireflection coated aspheric lens of focal length, 8mm, and a replica diffraction grating (on a copper substrate) with 600 lines/mm in the Littrow configuration to provide wavelength selective feedback and hence a means for tuning the lasing wavelength. The grating was blazed for a wavelength of 1.0μm and had reflectivities of ~90% (polarized perpendicular to the grooves) and 63%% (polarized parallel to the grooves) at 1.0-1.1μm. The fiber end facet nearest the grating was cleaved at an angle ~84º to the fiber axis in order to suppress broadband feedback from the uncoated face which might otherwise compete with the wavelength-dependent feedback provided by the grating and thus restrict the tuning range. The pump in-coupling end of the fiber was cleaved perpendicularly to provide the feedback necessary for laser oscillation. This end of the fiber also

served as the output coupler and, due to its high transmission (~96.4%), dominates over the feedback losses at the grating end of the laser. The fiber laser output was extracted by means of a dichroic mirror with high reflectivity (>99%) in the range 1.035-1.15μm and high transmission (87%) at the pump wavelength, inclined at a small angle with respect to the pump beam. With this arrangement the maximum pump powers incident and launched into the Yb-doped fiber were 380W and 150W respectively.

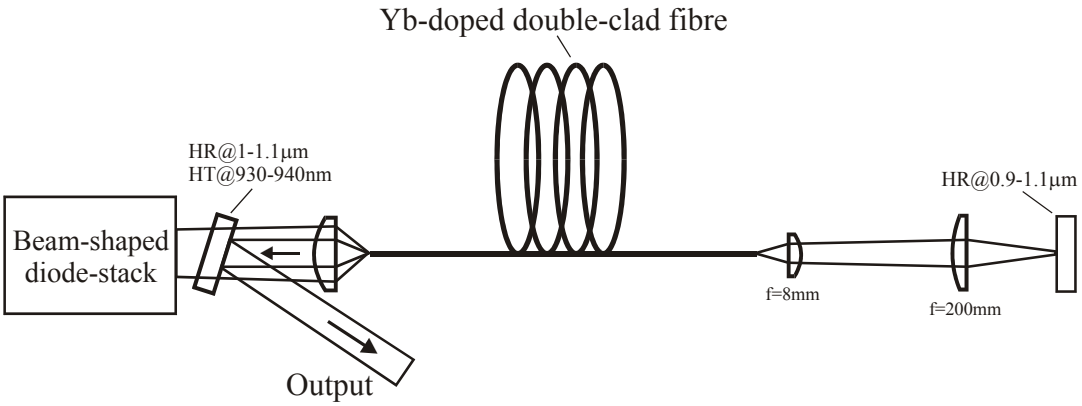


Figure 21: Laser set-up for diode-stack pumped Yb-doped straight-offset-core fiber laser.

Prior to operating the Yb-doped fiber laser in the tunable resonator configuration (figure 21), preliminary experiments were conducted on a simple Yb fiber laser with feedback for lasing provided by ~3.6% Fresnel reflections from perpendicularly-cleaved facets at both ends of the fiber to determine the maximum efficiency attainable from the tunable Yb fiber laser and to determine an approximate value for the background core propagation loss. The maximum length of fiber available for our experiments was ~14m. The effective absorption coefficient for the fiber at 940nm was determined via the cut-back technique to be 0.42dB/m, and hence ~74% of the launched pump power was absorbed in the fiber. The Yb fiber laser reached threshold at an absorbed pump power of <3W and at the maximum available pump power (corresponding to ~112W absorbed) yielded a combined output power (i.e. from both ends) of 80.4W, corresponding to a slope efficiency of ~74%. Based on the value for slope efficiency, we estimate that the core propagation loss is <0.05dB/m.

For the tunable Yb fiber laser configuration using the same fiber we obtained a maximum output power in the 1070-1074nm wavelength regime of 68W and a corresponding slope efficiency with respect to absorbed power of 63% (see Figure 22). The decrease in efficiency compared to the non-tunable fiber laser configuration indicates that the effective feedback reflectivity of the external cavity is ~45%. This is somewhat lower than expected based on the grating reflectivity and losses in the collimating lens, and hence is most probably due to imperfect alignment of the collimating lens and/or grating. The fiber laser operating wavelength could be adjusted via a simple adjustment of the grating angle. In preliminary experiments to determine the extent of the

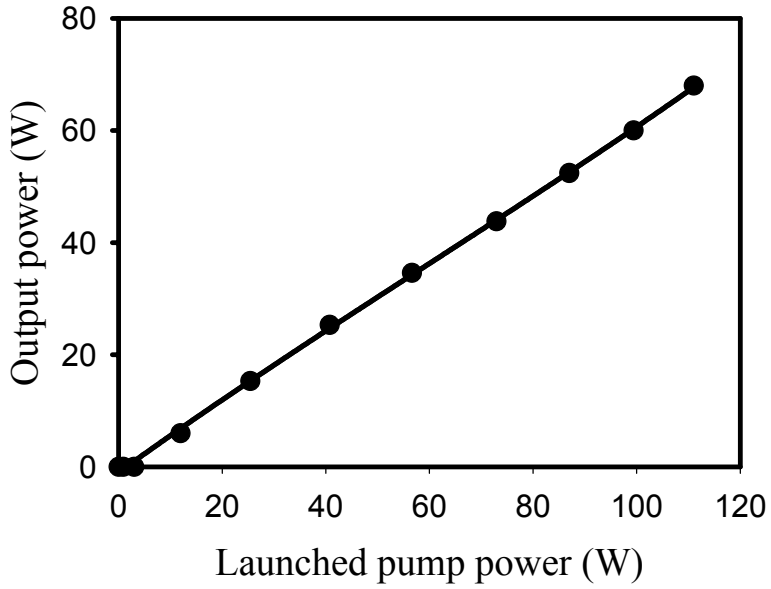


Figure 22: Output power of Yb-doped straight-offset-core fiber laser versus launched pump power.

tuning range it was found that Yb-doped fiber end facets were susceptible to damage when the lasing wavelength was adjusted to the upper and lower limit of the tuning range. One possible explanation for this behaviour is the occurrence more pronounced self-pulsing due to the presence a higher inversion density and hence greater stored energy at the limits of the tuning range. For this reason tuning experiments were generally performed at slightly lower pump powers and great care was taken not to extend the lasing wavelength to regions where the output power was significantly reduced. Figure 23 shows the output power as a function of lasing

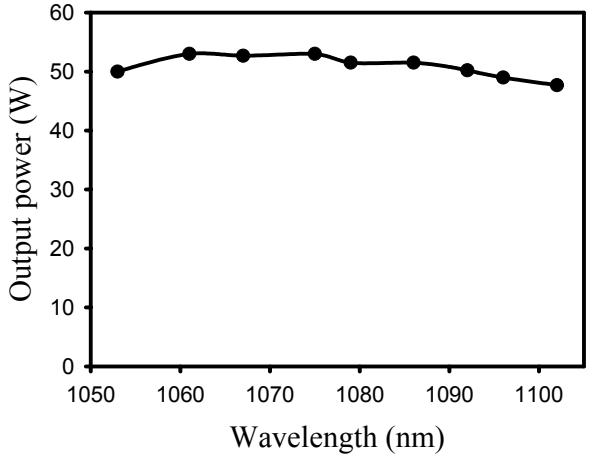


Figure 23: Output power versus laser wavelength for tunable laser configuration.

wavelength for an absorbed pump power of ~99W. The laser yielded >48W output power over a wavelength tuning range of 49nm from 1053nm to 1102nm with a linewidth of <2nm. The maximum output power (~53W) was obtained at a wavelength of ~1070 - 1075nm, but there is only a very small variation in the output power (<10%) over the most of the tuning range. This is an attractive feature of cladding-pumped fiber lasers and a consequence of being able to pump at power levels very many times the threshold pump power. At the maximum output power only ~3W of power was reflected from the grating into the zero-order. There was no evidence of self-pulsing behaviour and the short term power stability was relatively good (< ±5%). These results suggest that with an improved wavelength selection scheme deliberately operating the fiber at shorter wavelengths may well prove to be an attractive method for raising the thermally-induced damage limit.

## 8.0 Modeling of the loss in helical core fibers

In addition experimental work aimed at determining the optimum parameters (pitch and core-offset) for a helical-core fiber (as described in the previous sections), we have also found that Marcuse's model [6,7] for bend loss applied to helical-core fibers gives values for helical loss that agree reasonably well with some of our earlier results. The model that we have used is based on the following papers by Marcuse published in *Journal of Optical Society America* in 1976.

Paper 1. "Curvature loss formula for optical fibers" [6]

This paper gives the general formula for curvature loss in optical fibers, assuming an infinite cladding and ignoring the effect of field deformation caused by the curved axis of the fiber. The bend loss coefficient $\gamma$ is given by

$$\gamma = \frac{1}{\rho}\left(\frac{\pi\rho}{R_b}\right)^{1/2} \cdot \frac{U^2}{e_v V^2 W^{3/2} K_{v-1}(W) K_{v+1}(W)} \cdot \exp\left(-\frac{2\beta R_b W^3}{3(knc\rho)^3}\right) \qquad (4)$$

where $e_v$=2 if $\nu$=0 ($LP_{01}$, fundamental mode) and otherwise $e_v$=1 (i.e. for higher order modes, such as $LP_{v1}$ mode), U, V, and W are the waveguide modal parameters, K(W) is the modified Hankel function of W, $\beta$ is the propagation constant of the mode in the fiber, k is the free space propagation constant, $\rho$ is the fiber core radius and $R_b$ is the bend radius of the fiber.

Paper 2. "Radiation loss of a helically deformed optical fiber" [7]

This paper shows that the loss formula for a core with a helical trajectory agrees with the curvature loss formula (4) for a circularly deformed fiber if the radius of curvature of the circle is replaced by the radius of curvature of the helical trajectory. In other words, the propagation loss in a helical-core fiber can be estimated using loss formula (4) by replacing $R_b$ by $P^2/(4\pi^2 Q)$, where P is the pitch and Q is the core-offset.

Marcuse's model is suitable for estimating bend losses for the fundamental mode and higher-order modes in single/multi-mode fibers, while the model derived by Love and Snyder [7] is based on "thin wire" approximation which is only accurate for calculating the curvature loss for the fundamental-mode in single-mode fibers.

Using Marcuse's model, we have calculated the helical-loss for the $LP_{01}$ and $LP_{11}$ modes in the Yb-doped helical-core fibers and undoped helical-core fibers discussed in earlier section of the report, and we compared the values with our experimental results.

Case 1: Undoped helical-core fiber with pitches: 3.5mm; 4mm; 4.5mm and 5mm, NA 0.14, core offset = 120μm and core diameter 10μm.

The "cutback" method described in Section 3.3.1 was used to measure the fundamental mode propagation loss in these fibers at 1064nm and at 633nm using probe beams from Nd:YAG and He-Ne lasers respectively. The results (summarised in Table 5) show that the calculated loss values are very close to the measured values at 1064nm, but are not in such good agreement at 633nm.

| Nd:YAG: wavelength 1064nm | | | HeNe: wavelength 633nm | | |
|---|---|---|---|---|---|
| Pitch (mm) | Calculated (dB/m) | Measured (dB/m) | Pitch (mm) | Calculated (dB/m) | Measured (dB/m) |
| 4 | 46 | >50 | 3.5 | 5.4 | ~44 |
| 4.5 | 1.6 | ~2.5 | 4 | 0.13 | 0.26 |
| 5 | 0.04 | <0.3 | 4.5 | 0 | <0.3 |

Table 5: Calculated and measured propagation losses of helical-core fibers.

Case 2: Yb-doped single-clad helical-core fibers with pitches in the range 4 - 8mm, core offset = 130μm, NA=0.143, core diameter = 26μm.

These fibers were used in our core-pumped helical-core fiber laser experiments described in Section 3.5. The calculated loss (dB/m) versus pitch for $LP_{01}$ and $LP_{11}$ modes is shown in figure 24. For fibers with pitches of 4.0mm and 4.55mm, the losses for both $LP_{01}$ and $LP_{11}$ modes are very high (>1000dB/m), thus explaining why it was not possible to achieve lasing in these fibers. For the 5.17mm pitch fiber, the loss for the $LP_{01}$ mode is several dB/m, while the loss for $LP_{11}$ is >1000dB/m. We obtained robust single-mode laser operation for this fiber, but the efficiency was rather low because of the relatively high loss the fundamental mode. For pitches of 6.12mm and 7.14mm, the losses for $LP_{01}$and $LP_{11}$ are less than 0.2dB/m. Both of these fibers produced a multimode laser output due to there being insufficient suppression of higher order modes. The $M^2$ for the 6.12mm and 7.14mm pitch fiber lasers were measured to be 1.25 and 1.8 respectively. The above discussion suggests that calculated losses agree very well with the results for laser performance. From the model, the ideal pitch for this YHF should be in the range of 5.2mm~6mm.

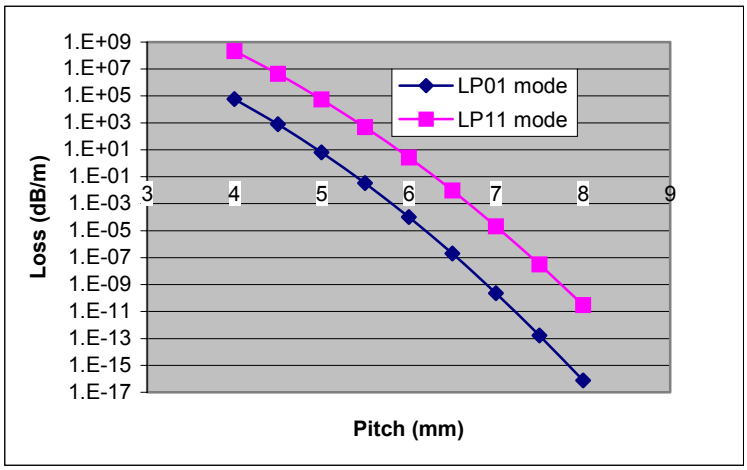


Figure 24: Loss of $LP_{01}$ and $LP_{11}$ mode versus pitch for Yb-doped helical-core fibers.

# 9.0 Cladding-pumped helical-core fiber lasers and amplifiers

## 9.1 Cladding-pumped Yb-doped helical-core fiber laser

A 'top-hat' refractive index profile for the core in combination with the correct helical core geometry is essential for efficient operation on the fundamental mode ($LP_{01}$) in a large core fiber device. After a considerable amount of effort targeted at improving the preform fabrication procedure we can now fabricate Yb-doped large core fibers with a nearly 'top-hat' index profile and with a relatively low core NA for the purpose of reducing the pump propagation loss. For this preliminary proof-of-principle study the core diameter, core NA, core offset and inner-cladding diameter were 30µm, 0.087, 100µm and 275µm respectively. The core NA is much less than for the fibers used in our previous experiments. The fiber was coated with a low refractive index polymer outer-cladding to provide a high numerical aperture of ~0.49 (calculated) for the inner-cladding pump guide. Fibers with a range of pitches (8.0mm, 8.3mm, 8.5mm, 8.8mm, 9.2mm and 9.6mm) were fabricated by careful adjustment of the preform spinning speed. These pitches were chosen to yield propagation losses for the $LP_{01}$ (fundamental) and $LP_{11}$ modes (calculated using the analysis described in section 3.7) in the regime of interest for efficient operation on the $LP_{01}$ mode and suppression of higher order modes (see figure 26). The results of this analysis suggested that helical-core fibers with pitches between ~8.5mm and ~8.8mm would perform best having a relatively low propagation loss (<0.6dB/m) for the $LP_{01}$ mode and a relatively high propagation loss (>9dB/m) for the $LP_{11}$ mode. In addition, a straight-core fiber with the same core and cladding dimensions was pulled from the preform (i.e. without spinning) to allow a direct comparison between the performance of the helical-core and straight-core fiber lasers.

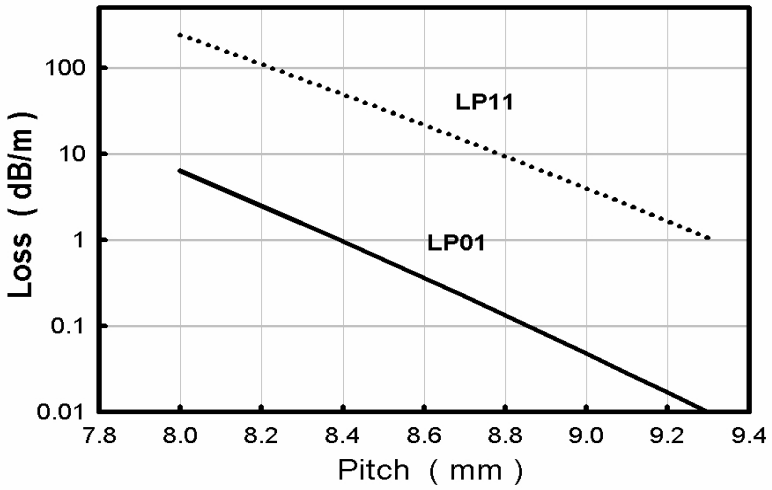


Figure 26: Calculated propagation loss for the $LP_{01}$ and $LP_{11}$ modes versus pitch.

The double-clad Yb-doped helical-core and straight-core fibers were tested in the laser configuration shown in figure 27. A relatively simple resonator design was employed consisting of a length of the fiber under investigation with feedback for lasing provided by a cleaved fiber end facet (also serving as the output coupler) at the pump in-coupling end of the fiber and, at the opposite end of the fiber, by an external cavity comprising an 8mm focal length aspheric collimating lens, a 100mm focal length focussing lens and a plane mirror with high reflectivity (>99%) over the wavelength range 0.9μm–1.1μm. It should be noted that light emerges from a perpendicularly-cleaved end facet on a helical-core fiber at an angle (arc[nsin($\theta_i$)]) to the fiber axis, which, in the case of the 8.5mm pitch fiber, is ~6º. Hence, careful alignment of the external feedback cavity lenses and mirror at the appropriate angle to the fiber is required to avoid a reduction in the feedback efficiency. There is also a reduction in the feedback efficiency at the pump in-coupling end of the fiber due to the angle of the core relative to the cleaved facet, but the feedback efficiency is still sufficient for efficient laser oscillation with the relatively high pump power available in our experiment. The pump light was provided by the 976nm diode-stack source and was coupled into the fiber with the aid of two 30mm focal length aspheric lenses. With this arrangement a maximum of 120W of pump could be launched into the fiber. However for the experiments described here, no attempt was made to actively cool the fiber, so the pump power was limited to <95W to reduce the risk of damage. The pump absorption efficiency was determined via a cut-back measurement to be 5.8dB/m. This allowed a relatively short length of fiber (~2.8m) to be used for efficient pump absorption. The fiber laser output was extracted with the aid of a dichroic mirror (as shown).

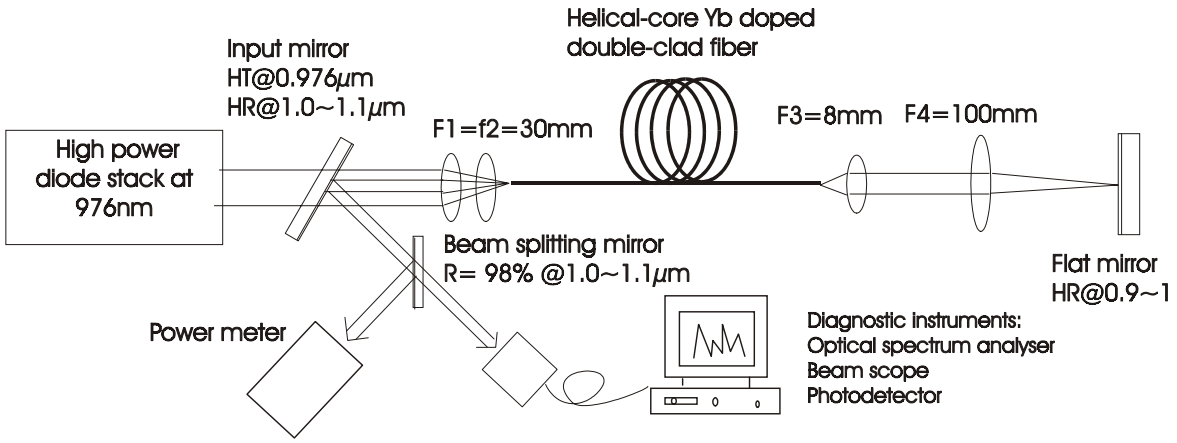


Figure 27: Cladding pump Yb-doped helical-core fiber laser arrangement

The best performance was obtained with the 8.5mm pitch fiber. The fiber laser reached threshold at a launched pump power of ~10W and yielded 60.4W of output for 92.6W of launched pump power (see figure 28). At pump powers well above threshold, the slope efficiency reached ~84%, which compares favourably with the best slope efficiencies routinely achievable with more conventional straight-core Yb-doped double-clad fiber lasers. The centre lasing wavelength and emission linewdith were 1043nm and 9nm respectively (see figure 29). The former was a little shorter than is typical for cladding-pumped Yb-doped fiber lasers due to a combination of relatively short fiber length (i.e. with lower re-absorption loss) and reduced 'helical' loss at shorter wavelengths.

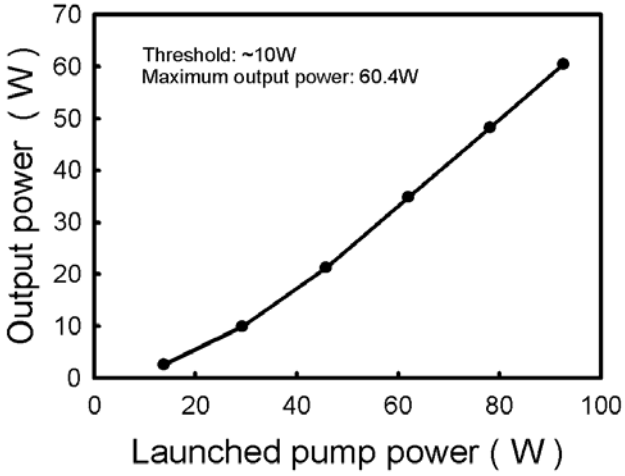


Figure 28: Output power versus launched pump power for the 8.5mm pitch fiber.

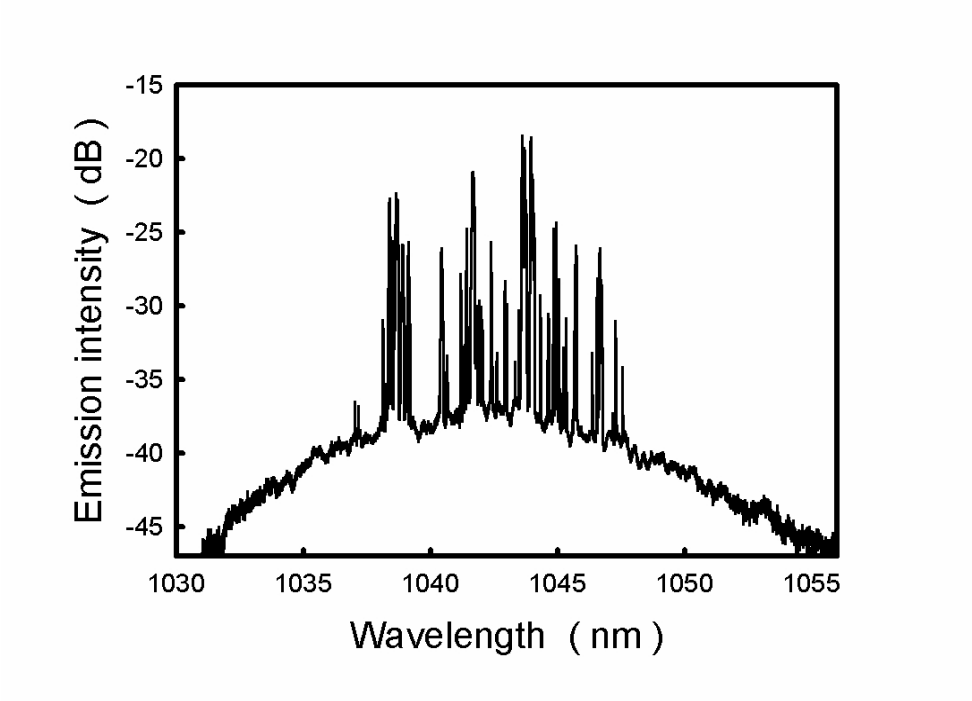


Figure 29: Emission spectrum of helical core fiber laser.

The beam quality factor $M^2$ was measured using a Dataray® Beamscope and found to be <1.4 at highest output power level. The beam profile (shown in figure 30(a)) confirms the single-mode nature of the output beam. In contrast, the output beam from the Yb-doped straight-core fiber laser was found to be multimode with $M^2 \approx 3.6$ (see figure 30(b)) and the lasing wavelength was much longer with emission lines around 1050nm and 1080nm.

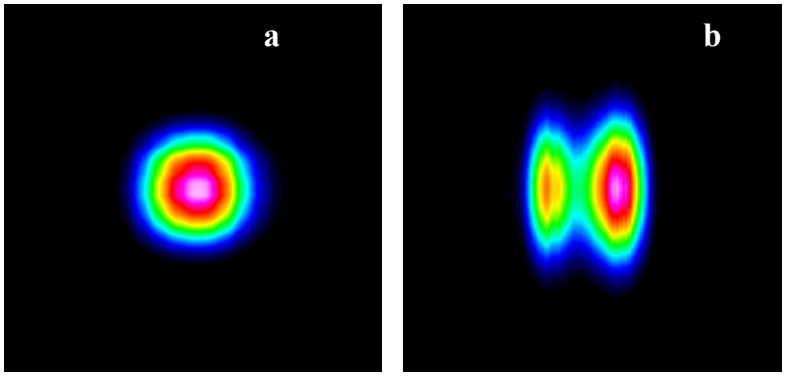


Figure 30: (a) Beam profile for 8.5mm pitch helical-core fiber laser, and (b) beam profile for straight-core fiber laser

The calculated values for propagation loss versus pitch (shown in figure 26) suggest that 8.8mm pitch fiber should have provided the best performance with a relatively low loss (0.13dB/m) for the $LP_{01}$ mode and a high loss (9.4dB/m) for the $LP_{11}$ mode. This fiber, when tested in the laser configuration shown in figure 27, did in fact produce a single-mode output at low powers, but the beam quality degraded to $M^2 \approx 1.7$ at an output power of 40W indicating that there was insufficient loss to discriminate against higher-order modes. In contrast, the 8.5mm pitch fiber had a higher efficiency than was expected based on the calculated value for the propagation loss for the $LP_{01}$ mode of 0.6dB/m. These results indicate that the model [6, 7] slightly over-estimates the propagation losses, but is nevertheless a very useful design aid for helical-core fiber lasers and amplifiers. According to the model, the helical-loss is also dependent on the signal wavelength. For example, for the 8.5mm pitch fiber we calculate that the helical-loss for the $LP_{01}$ mode is 0.59dB/m and 1.0dB/m at wavelengths of 1040nm and 1100nm respectively. In practice, the values for helical-loss are somewhat lower, as confirmed by our results for laser performance, but reduced helical-loss at shorter wavelengths still favours laser operation at shorter wavelengths. This may well prove to be an extremely important feature of helical-core fiber lasers since efficient operation at shorter wavelengths will lead to reduced quantum defect heating and hence will facilitate further power scaling. It is also worth mentioning that the origin of the 'helical' loss in the regime in which we are operating is the same as for bend-induced loss in a coiled straight-core fiber. Thus, to achieve the same level of discrimination against higher-order modes in the straight-core fiber as in the 8.5mm pitch fiber would require coiling the straight-core fiber with a bend radius of 1.8cm. Clearly, this would be extremely difficult to achieve in a fiber with a large inner-cladding size (>500μm) selected for efficient in-coupling of higher pump power.

### 9.2 Cladding-pumped helical core fiber amplifier

The above fibers were also tested in a MOPA configuration, as shown in figure 31. Two single-mode laser sources were used as maser-oscillators: a tunable Yb fiber laser and an Yb:YAG laser. The laser wavelength of Yb:YAG laser was 1050nm and emission linewidth (FWHW) was ~1.0nm (see figure 32). A maximum output power of 5W was obtained from this laser with a beam quality factor ($M^2$) of less than 1.2. Using the 9.2mm pitch helical-core fiber in an amplifier configuration we obtained more than 92W of output with 143W of launched diode pumped power at 976nm corresponding to a slope efficiency of 73% (see figure 33). The $M^2$ parameter was measured to be 1.3 at an output power level of ~15W, but degraded to 2.13 at an output power of ~ 90W.

The set-up for the tunable Yb fiber laser is also shown in figure 31. In this case wavelength tuning was achieved using a simple external cavity containing a diffraction grating (600line/mm and blazed at 1μm). This laser yielded over 15W of output @1090nm and the lasing wavelength could be tuned (by adjusting the angle of the grating) from 1046nm to 1110nm with a 15m long piece of double-clad Yb-doped fiber. With a shorter length of fiber (~8m) a slightly extended tuning range from 1036nm to 1106nm could be achieved, but with a somewhat lower maximum output power of ~10W. The beam quality factor ($M^2$) was measured to be <1.07 and the emission linewidth was less than 0.3nm. This tunable fiber oscillator was used to seed a power amplifier based on a 2.8m length of the 8.5mm pitch double-clad Yb-doped helical-core fiber. In

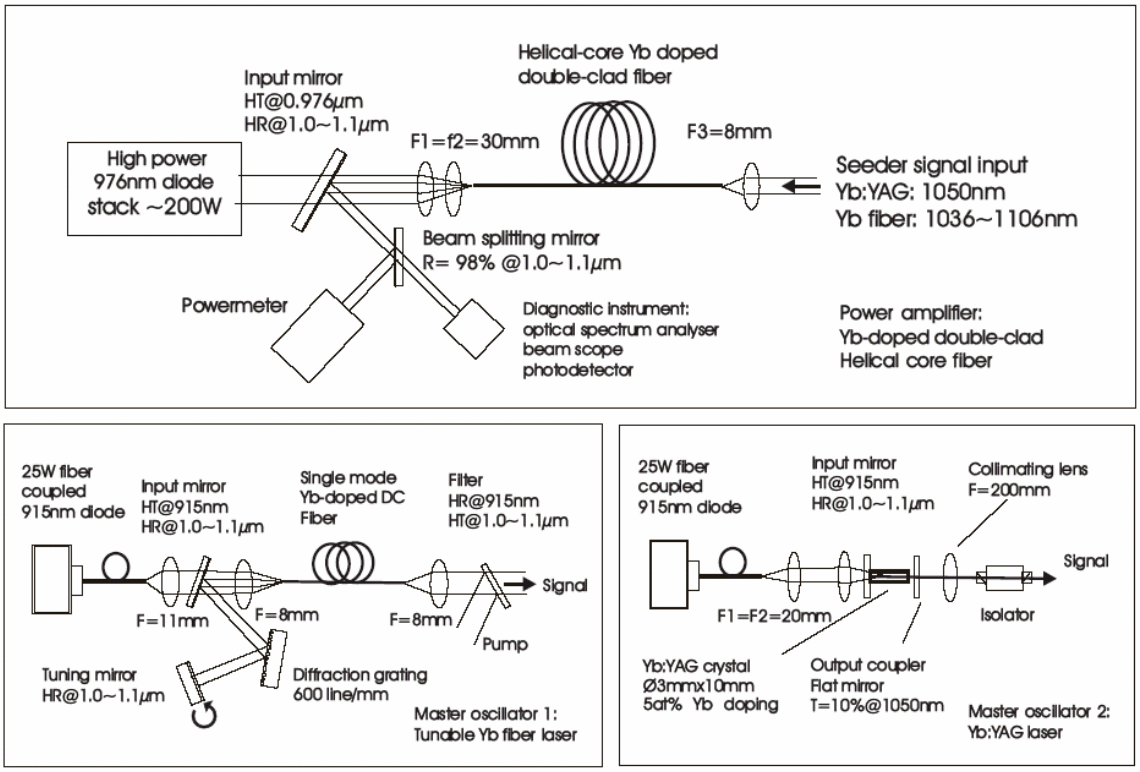


Figure 31: Set-up diagram for diode-pumped helical-core MOPA (1. Master oscillator - single mode tunable Yb fiber laser, 2. Master oscillator -single mode Yb: YAG crystal laser, 3. Helical-core power amplifier.

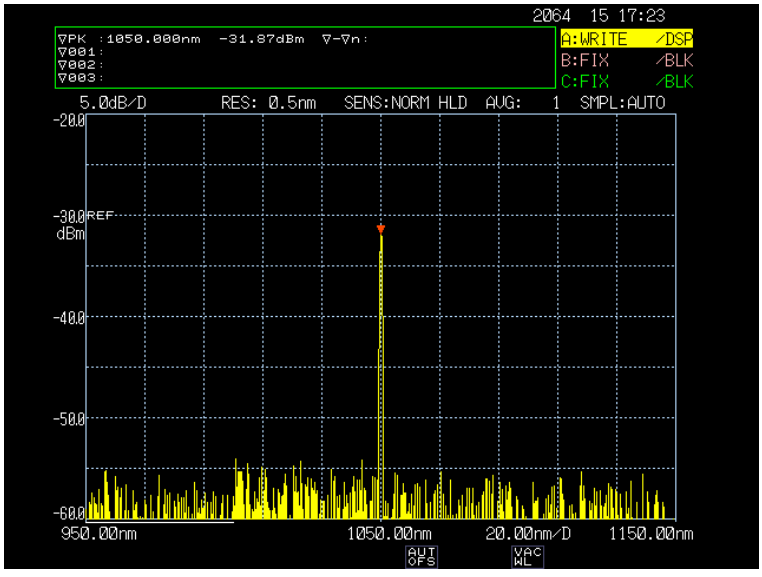


Figure 32: Emission spectrum from 9.2mm pitch helical fiber with Yb:YAG seed laser.

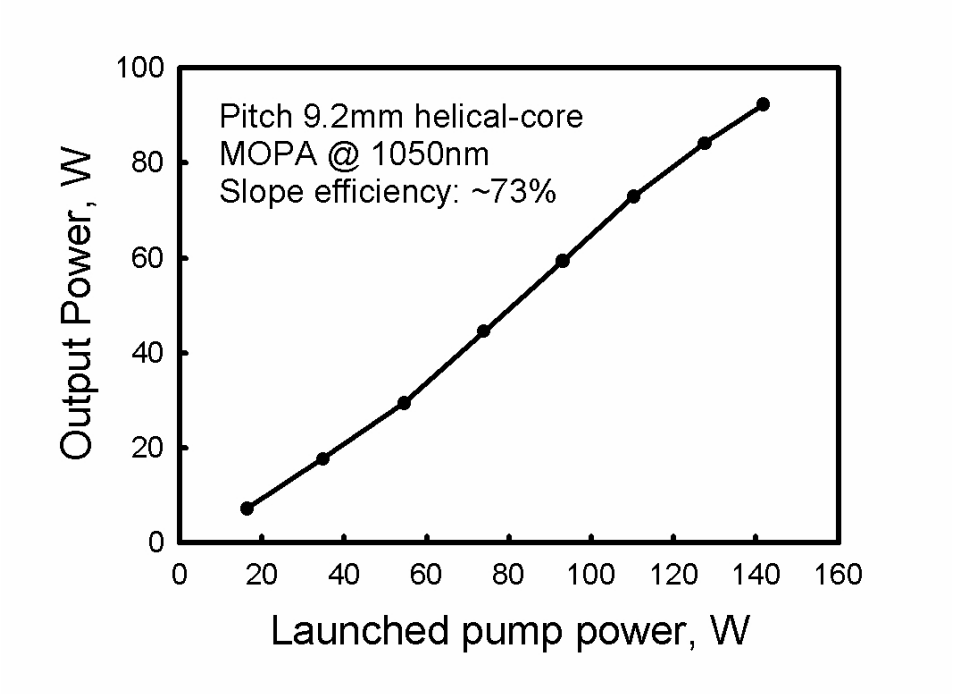


Figure 33: Output versus launched pump power for 9.2mm pitch helical core MOPA

this experiment the fiber oscillator wavelength was tuned to the emission peak for the helical-core fiber at 1043nm. For ~600mW of launched seed power, we obtained a maximum output power from the fiber amplifier of 40W for 62W of launched pump power. The slope efficiency at high pump powers was ~84% (see figure 34) and hence comparable to that obtained in the

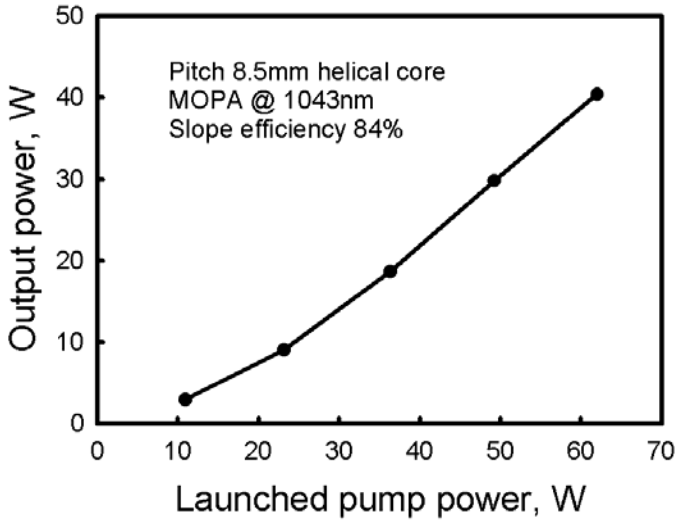


Figure 34: Output versus launched pump power for 8.5mm pitch helical core MOPA.

helical-core fiber oscillator described earlier. The maximum output power from the amplifier was limited by damage to one of the fiber end facets. The emission linewidth was measured to be less than 0.3nm (see figure 35) and hence the same as for the master-oscillator.

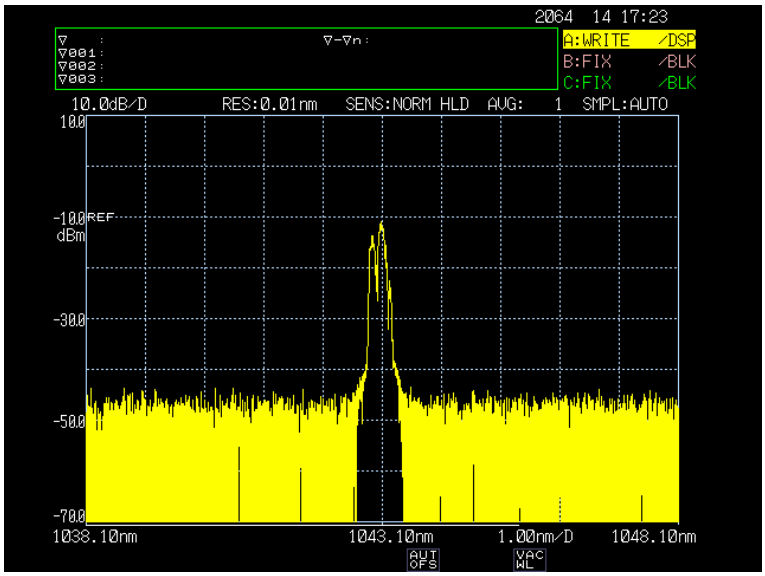


Figure 35: Emission spectra from helical core fiber amplifier (Pitch 8.5mm) seeded by the tunable Yb fiber laser.

## 10.0 Prospects for further power scaling

At present, the main factor limiting the maximum power available from the helical-core fiber lasers described in this report is the diode pump power that can be launched into the fibers. This problem can be solved by improving the design of the diode pump module to increase the pump brightness and/or by increasing the inner-cladding diameter.

### 10.1 Improving the diode-stack pump module

In the present design of pump module the beam quality factor in the stacking direction is over a factor-of-ten times larger than the theoretical limit. This is mainly due to pointing errors in the collimated beams from adjacent bars caused by imprecise positioning of the fast-axis collimating lenses. There scope for improving the beam quality factor in the fast-direction (and hence the brightness) by at least a factor-of-four by employing a better jig for aligning and fixing the microlenses in position.

### 10.2 Increasing the inner-cladding diameter of helical core fibers

A further increase in launched pump power can also be achieved by using a fiber with a larger inner-cladding diameter. However, it is also necessary to increase the core size and/or Yb doping concentration in order to keep the fiber device length reasonably short. Our modeling results indicate that it should still be possible to achieve efficient single-mode operation with core diameters as large as 50μm, and possibly larger diameters. For example, when the core diameter, NA, pitch and core offset are choose to be 50μm, 0.06, 22.1mm and 200μm respectively, the calculated losses for $LP_{01}$ and $LP_{11}$ modes are ~0.12dB/m and ~5dB/m respectively. In this case, the inner-cladding diameter of the fiber can be increased to be 600 micron allowing several kilowatt of pump power to be launched into the fiber. Thus, it should be possible to scale single-mode powers into the kW regime and beyond using a cladding-pumped helical-core fiber laser.

## 11.0 Conclusions and future work

We have shown that the use of a helical-core fiber geometry can be a very effective method for suppressing high order modes in a large-core fiber device, and hence is an attractive method for scaling of single-mode powers in fiber lasers and amplifiers. Using this approach we have successfully demonstrated efficient single-spatial-mode operation of core and cladding-pumped Yb-doped helical-large-core lasers. In the latter we obtained an output power of over 60W and the slope efficiency (>80%) was comparable with that routinely obtained in more conventional straight-core Yb-doped fiber lasers. It is clear that with relatively simple improvements in the fiber design, and with the availability of a higher power and higher brightness pump source, it should be possible to scale to significantly higher power levels whilst maintaining robust single mode operation. Precise control of the fiber parameters (e.g. index profile and pitch) is essential, and hence further refinement of the fabrication procedure will be needed to ensure success. The ability to use the helical-core geometry for suppression of higher-order modes in conjunction with a large inner-cladding design may well prove to be one of the few practical methods for ensuring single-mode operation in very high power fiber devices, where bending the fiber to a small radius as required in the conventional ‘bend-loss filtering’ approach is no longer possible.

The polarisation maintaining properties of helical-core fibers have been studied in some detail. Unfortunately, the fiber designs required for a high enough circular birefringence for polarisation maintenance also lead to a high pump propagation loss in cladding-pumped helical-core devices due to reflection from the core-cladding interface. At the moment, there is no obvious way to solve this problem. One possibility would be to employ a two stage fiber device, where the first stage is a cladding-pumped Yb-doped helical-core fiber laser designed to produce high-power single-mode (but unpolarised) output, which is used to core-pump a second helical-core fiber laser with a high circular birefringence in order to produce a polarised single-mode output. This is certainly one solution to the problem, but it suffers from the disadvantage that it is rather complicated.

In summary, we believe that helical-core fibers are attractive for power-scaling of single-mode operation, but do not appear to be very promising for polarisation maintenance.

## 12.0 References


1. J. P. Koplow, D. A. V. Kliner, L. Goldberg "Single-mode operation of a coiled multimode fiber amplifier", Opt. Lett., **25**, 442-444 (2000).
2. J. Limpert, A. Liem, H. Zellmer and A. Tunnermann "500-W continuous-wave fiber laser with excellent beam quality", Electron. Lett., **39**, 645-647 (2003).
3. Y. Jeong, J. K. Sahu, D. N. Payne, and J. Nilsson, "Ytterbium-doped large-core fiber laser with 1.36 kW continuous-wave output power," Opt. Express **12,** 6088-6092 (2004).
4. J. Qian and C. D. Hussey "Circular birefringence in helical-core fibre", Electron. Lett., **22**, 515-517 (1986).
5. W. A. Clarkson and D. C. Hanna, "Two-mirror beam-shaping technique for high-power diode bars", Opt. Lett., 21, (1996), 375
6. D. Marcuse, " Curvature loss formula for optical fibers", J. Opt. Soc. Am., Vol. 66, No. 3, pp216-220, 1976.
7. D. Marcuse, " Radiation loss of a helically deformed optical fiber", J. Opt. Soc. Am., Vol. 66, No. 10, pp1025-1031, 1976.
8. J. D. Love and A. W. Snyder, Electron. Lett., " Radiation from single-mode helical fibres", vol.23, (1987), p1109-1110
9. Y. E. Young, S. D. Setzler, K. J. Snell, P. A. Budni, T. M. Pollak and E. P. Chicklis, Opt. Lett., vol.29 (2004), p.1075
10. D. Y. Shen, A. Abdolvand, L. J. Cooper and W. A. Clarkson, Appl. Phys. B, vol.79 (2004), p.559


## 13.0 Publications


1. P. Wang, L. J. Cooper, W. A. Clarkson, J. Nilsson, R. B. Williams, J. K. Sahu and A. K. Vogel, " Helical-core ytterbium-doped fibre laser" CLEO/Europe, CL2-6-THU, 2003
2. W. A. Clarkson, L. J. Cooper, P. Wang, R. B. Williams and J. K. Sahu, "Power scaling concepts for fiber lasers", OSA Advanced Solid State Photonics, WA1, 2003
3. P. Wang, L. J. Cooper, V. Shcheslavskiy, J. K. Sahu and W. A. Clarkson, "Cladding-pumped ytterbium-doped helical-core fiber laser", OSA Advanced Solid State Photonics conference, 2005, MC5
4. P. Wang, L. J. Cooper, V. Shcheslavskiy, J. K. Sahu and W. A. Clarkson, "High power diode-pumped ytterbium-doped helical core fiber MOPA", submitted to Europe CLEO 2005
5. P. Wang, L. J. Cooper, R. B. Williams, J. K. Sahu and W. A. Clarkson, " Helical-core ytterbium-doped fibre laser", Electronics Letters, Vol. 40, No. 21, p1325-1326, 2004
6. W. A. Clarkson, P. Wang, L. J. Cooper and J. K. Sahu, " High-power tunable ytterbium-doped fibre laser pumped by a beam-shaped diode-stack", manuscript in preparation
7. P. Wang, L.J. Cooper, J. K. Sahu, W. A. Clarkson, " Single-mode operation of cladding pumped helical core ytterbium-doped fiber laser", manuscript in preparation
8. P. Wang L. J. Cooper, J. K. Sahu, W. A. Clarkson, " High power diode-pumped helical core MOPA", manuscript in preparation